CC chemokine receptor 4 is required for experimental autoimmune encephalomyelitis by regulating GM-CSF and IL-23 production in dendritic cells

Karola Poppensieker[a,1], David-Marian Otte[a,1], Britta Schürmann[a,b,1,2], Andreas Limmer[c], Philipp Dresing[d], Eva Drews[a], Beatrix Schumak[e], Luisa Klotz[c,f,3], Jennifer Raasch[g], Alexander Mildner[g,4], Ari Waisman[h], Stefanie Scheu[d], Percy Knolle[c], Irmgard Förster[i], Marco Prinz[g], Wolfgang Maier[b,j], Andreas Zimmer[a], and Judith Alferink[a,b,5]

[a]Institute of Molecular Psychiatry, Departments of [b]Psychiatry and [f]Neurology, [c]Institutes of Molecular Medicine and Experimental Immunology, and [e]Institute of Medical Microbiology, Immunology, and Parasitology, University of Bonn, 53127 Bonn, Germany; [d]Institute of Medical Microbiology and Hospital Hygiene, University of Düsseldorf, 40225 Düsseldorf, Germany; [g]Institute of Neuropathology, BIOSS Centre for Biological Signalling Studies, University of Freiburg, 79106 Freiburg, Germany; [h]Institute for Molecular Medicine, University Medical Center of Johannes Gutenberg University Mainz, 55131 Mainz, Germany; [i]Molecular Immunology, IUF-Leibniz Research Institute for Environmental Medicine, Heinrich Heine University, 40021 Düsseldorf, Germany; and [j]German Center for Neurodegenerative Diseases (DZNE), 53175 Bonn, Germany

Edited by Lawrence Steinman, Beckman Center for Molecular Medicine, Stanford, CA, and accepted by the Editorial Board January 19, 2012 (received for review September 1, 2011)

Dendritic cells (DCs) are pivotal for the development of experimental autoimmune encephalomyelitis (EAE). However, the mechanisms by which they control disease remain to be determined. This study demonstrates that expression of CC chemokine receptor 4 (CCR4) by DCs is required for EAE induction. CCR4$^{-/-}$ mice presented enhanced resistance to EAE associated with a reduction in IL-23 and GM-CSF expression in the CNS. Restoring CCR4 on myeloid cells in bone marrow chimeras or intracerebral microinjection of CCR4-competent DCs, but not macrophages, restored EAE in CCR4$^{-/-}$ mice, indicating that CCR4^{+} DCs are cellular mediators of EAE development. Mechanistically, CCR4$^{-/-}$ DCs were less efficient in GM-CSF and IL-23 production and also T_H-17 maintenance. Intraspinal IL-23 reconstitution restored EAE in CCR4$^{-/-}$ mice, whereas intracerebral inoculation using IL-23$^{-/-}$ DCs or GM-CSF$^{-/-}$ DCs failed to induce disease. Thus, CCR4-dependent GM-CSF production in DCs required for IL-23 release in these cells is a major component in the development of EAE. Our study identified a unique role for CCR4 in regulating DC function in EAE, harboring therapeutic potential for the treatment of CNS autoimmunity by targeting CCR4 on this specific cell type.

chemokines | neuroinflammation

Multiple sclerosis (MS) is a chronic demyelinating disease of the human CNS (1). Experimental autoimmune encephalomyelitis (EAE), the animal model of MS, is mediated by myelin-specific CD4^{+} T cells activated by professional antigen-presenting cells (APCs) in peripheral lymphoid tissues (2, 3). In recent studies, both peripherally derived macrophages and DCs have been shown to present myelin antigens to invading autoreactive T cells in the CNS. This presentation initiates the recruitment of a second wave of leukocytes that damage the target organ via demyelination and axonal degeneration (4–8). Understanding the mechanisms responsible for the recruitment of APCs to the CNS and their local function is essential for the development of therapeutic strategies targeting the effector phase and thereby controlling disease progression.

Chemokines and their G protein-coupled receptors are key regulators of leukocyte trafficking (9, 10). The CC chemokine receptor 4 (CCR4) is the cognate receptor for the CC chemokines CCL17 and CCL22, and is expressed on functionally distinct subsets of T cells, including activated T cells, T_H2 cells, and Treg cells. CCR4 has also been found on platelets, NK cells, macrophages, and DCs (11–15). DCs are important cellular sources for CCL17 and, in concert with macrophages, produce CCL22 during both homeostasis and inflammation (16, 17). Different studies have suggested a critical role for CCR4 in the pathogenesis of EAE and MS. For example, elevated levels of the CCR4 ligands CCL17 or CCL22 have been found in the cerebrospinal fluid of MS patients (18–20). CCL22 protein has been identified in CNS-infiltrating leukocytes and microglia of EAE-induced mice, and CCR4 is expressed by invading leukocyte subsets (21, 22). However, it remained undefined which CCR4-expressing cell population mediates its role in the development of CNS autoimmunity. Expression of CCR4 on APCs suggests that APC-dependent mechanisms may be involved in EAE and MS.

Recent studies have demonstrated an impact of CCR4 and its ligands on basic APC functions. For example, the rapid binding of antigen-primed T cells to activated DCs was dependent on CCR4, and the duration of their cognate interaction correlated with increased CCL17 production by DCs (23, 24). In addition, it was shown that CCL17 and CCR4 are implicated in facilitating a natural killer (NK) T cell-dependent way of licensing DCs for cross-priming (25). Furthermore, the release of proinflammatory cytokines and chemokines upon Toll-like receptor (TLR) engagement has been associated with CCR4 regulation (26).

In this study we sought to identify the essential CCR4-expressing cells mediating induction of EAE following myelin oligodendrocyte glycoprotein (MOG) peptide p35–55 immunization. We used a CCR4 knockout (CCR4$^{-/-}$) mouse model, transfer of encephalitogenic lymphocytes, generation of mixed BM chimeras, and the stereotactic CNS inoculation of myeloid cells to decipher the CCR4-dependent underlying molecular mechanisms required for disease susceptibility. Our data identified CCR4^{+} DCs, rather than macrophages or T cells, as the key mediators in the development of EAE. We now show that GM-CSF–dependent IL-23 production in DCs was dependent on CCR4 expression in these cells and required for development of EAE. This functional role for CCR4 in the effector phase of disease points toward a unique strategy to inhibit CNS autoimmunity by targeting this chemokine receptor on DCs.

Author contributions: K.P., D.-M.O., B. Schürmann, A.L., S.S., W.M., A.Z., and J.A. designed research; K.P., D.-M.O., B. Schürmann, A.L., P.D., B. Schumak, L.K., J.R., S.S., M.P., and J.A. performed research; A.W., P.K., and I.F. contributed new reagents/analytic tools; K.P., D.-M.O., B. Schürmann, A.L., P.D., B. Schumak, L.K., J.R., S.S., M.P., and J.A. analyzed data; and K.P., D.-M.O., B. Schürmann, A.L., E.D., A.M., S.S., P.K., A.Z., and J.A. wrote the paper.

The authors declare no conflict of interest.

This article is a PNAS Direct Submission. L.S. is a guest editor invited by the Editorial Board.

[1]K.P., D.-M.O., and B. Schürmann contributed equally to this work.

[2]Present address: Department of Physiology, Feinberg School of Medicine, Northwestern University, Chicago, IL 60611.

[3]Present address: Department of Neurology, University of Münster, 48149 Münster, Germany.

[4]Present address: Department of Immunology, The Weizmann Institute of Science, Rehovot 76100, Israel.

[5]To whom correspondence should be addressed. E-mail: judith.alferink@ukb.uni-bonn.de.

This article contains supporting information online at www.pnas.org/lookup/suppl/doi:10.1073/pnas.1114153109/-/DCSupplemental.

Results

CCR4 Deficiency in Hematopoietic Cells Confers EAE Resistance. To determine the expression of CCR4 during EAE, C57BL/6 mice were immunized with $MOG_{35–55}$ peptide (hereafter referred to as MOG) in complete Freund's adjuvant (CFA), and quantitative PCR analysis on CNS tissues was performed. At the peak of disease (day 17 after MOG immunization), CCR4 mRNA levels in the spinal cords were significantly increased; and they declined with the remission of neurological symptoms 34 d after immunization (Fig. 1*A*). We found high CCR4 expression in $CD4^+$ T cells isolated from the CNS, in contrast to low levels in $CD11b^+$ cells comprising macrophages/microglia and DCs (Fig. S1*A*). In accordance, flow cytometry detected higher CCR4 surface levels on $CD4^+$ T cells compared with myeloid-derived cells, both of which immigrated into the CNS as identified by high expression of the hematopoietic marker CD45 (Fig. S1*B*). Microglial cells ($CD45^{low}$ $CD11b^+$) did not express CCR4.

To evaluate the contribution of CCR4 expression on myeloid vs. lymphoid cells to EAE pathogenesis we used a $CCR4^{-/-}$ mouse model. After MOG immunization, WT mice developed severe EAE, whereas $CCR4^{-/-}$ mice only showed mild clinical signs with significantly diminished incidence of disease and mean maximal clinical scores (Fig. 1*B* and Table S1). In addition, immunohistochemistry of $CCR4^{-/-}$ spinal cord sections collected at day 35 showed a reduced infiltration of T cells, macrophages, and B cells, as well as a diminished demyelination and neurodegeneration (Fig. 1*C* and Fig. S1*C*). Consistent with these results, flow cytometry analyses at peak disease (day 17) detected reduced numbers of $CD4^+$ T cells, $CD11b^+$ macrophages, and MHC class II^+ cells, as well as diminished IL-17–and IFN-γ–producing $CD4^+$ T cells in the $CCR4^{-/-}$ CNS (Fig. 1 *D* and *E* and Fig. S1 *D–F*).

To identify the $CCR4^+$ cell population relevant to EAE induction, bone marrow (BM) chimeric mice were generated (Fig. 1*F* and Table S2). Lethally irradiated CD45.1 WT mice were reconstituted with BM cells from either CD45.2-expressing $CCR4^{-/-}$ mice ($CCR4^{-/-}$→WT) or WT mice (WT→WT). $CCR4^{-/-}$→WT chimeras containing immune cells of hematopoietic origin that did not express CCR4 showed resistance to EAE, whereas WT→WT chimeras exhibited severe clinical symptoms after MOG immunization. To exclude a role of CCR4 on CNS-resident cells during EAE, we transferred BM cells from WT to lethally irradiated $CCR4^{-/-}$ mice (WT→$CCR4^{-/-}$). As seen in Fig. 1*G*, WT→$CCR4^{-/-}$ mice developed severe EAE after MOG immunization comparable to WT→WT controls. These data indicate that EAE induction requires CCR4 expression on BM-derived cells, but not on CNS-resident cells.

$CCR4^{-/-}$ Mice Generate Encephalitogenic T Cells but Are Resistant to Passive EAE. Resistance to EAE in $CCR4^{-/-}$ mice could be caused by an intrinsic defect in generating encephalitogenic T cells. Therefore, we next investigated antigen-specific proliferation and T_H-1 or T_H-17 differentiation of $CD4^+$ T cells in the absence of CCR4. For this, $CD4^+$ T cells from $CCR4^{-/-}$ or WT mice were cultured under T_H-1 or T_H-17 differentiation conditions in vitro. Equal percentages of IFN-γ– or IL-17–producing cells were detected by flow cytometry in both cultures (Fig. S2*A*). In addition, $CD4^+$ T cells isolated from $CCR4^{-/-}$ mice at the priming phase (10 d after immunization) proliferated in response to MOG peptide to the same extent as WT $CD4^+$ T cells (Fig. S2*B*). Furthermore, percentages of IFN-γ– or IL-17 cytokine-producing T cells were equivalent in the spleens of $CCR4^{-/-}$ and WT cells at the priming phase (Fig. S2*C*).

We then asked whether MOG-reactive $CD4^+$ T cells generated in $CCR4^{-/-}$ mice were able to induce EAE upon adoptive transfer. To rule out a preferential role for CCR4 on T_H-1 vs. T_H-17 cells, we restimulated $CD4^+$ T lymphocytes from immunized WT and $CCR4^{-/-}$ mice with or without mouse IL-12 (IL-12). An equivalent T_H-1 shift with enhanced numbers of IFN-γ–producing cells and high IFN-γ, but low levels of IL-17 protein secreted was found in WT and $CCR4^{-/-}$ $CD4^+$ T cells cultured with IL-12 (Fig. S2 *D* and *E*). In contrast, in the absence of IL-12, MOG-reactive $CD4^+$ T cells produced IL-17 but reduced levels of IFN-γ (Fig. S2 *D* and *E*). WT mice injected with $CCR4^{-/-}$ or WT T_H-1 cells developed EAE with a comparable incidence and severity (Fig. 2*A*). Transfer of primed WT or $CCR4^{-/-}$ T lymphocytes containing T_H-17 cells induced only a mild EAE, but with equivalent clinical scores in WT recipients (Fig. S2*F*). Thus, CCR4 is not required in a cell-autonomous way on MOG-reactive $CD4^+$ T cells for the induction of EAE in naïve recipients.

Based on these results, we hypothesized that CCR4 does not play a role during the induction phase but rather during the effector stage of disease, i.e., within the CNS. Therefore, the course of EAE was compared in $CCR4^{-/-}$ and WT animals following the adoptive transfer of MOG-reactive WT lymphocytes. WT mice developed severe clinical EAE (Fig. 2*B*), whereas $CCR4^{-/-}$ mice exhibited resistance to EAE. Thus, for disease susceptibility,

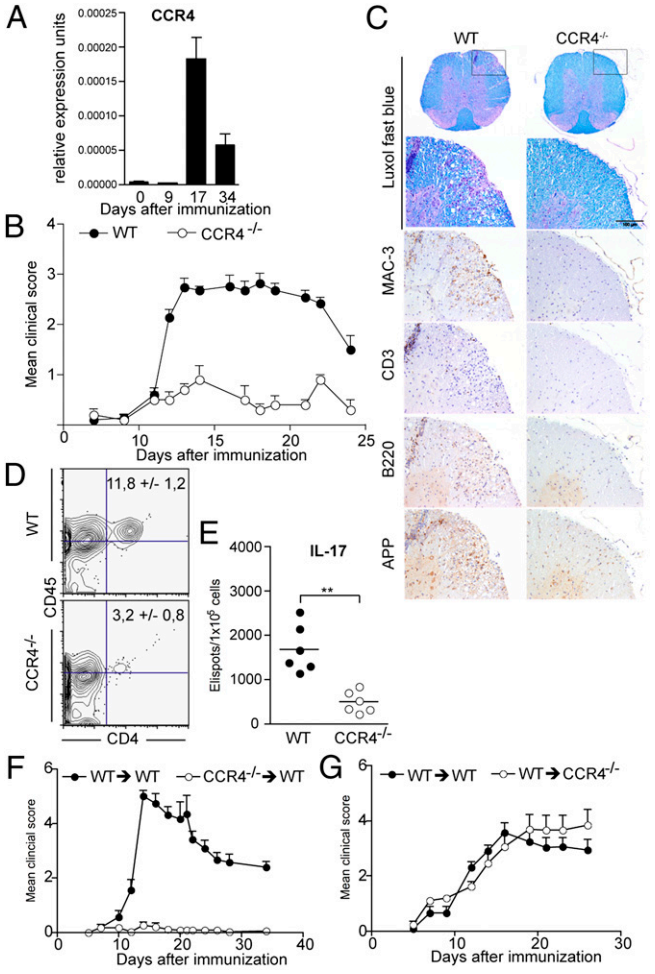

Fig. 1. CCR4 deficiency in hematopoietic cells confers EAE resistance. (*A*) Real-time PCR analysis of CCR4 mRNA expression in the CNS of MOG-immunized C57BL/6 mice (n = 3–5 mice per group). mRNA levels are normalized to GAPDH expression, and results are presented as mean ± SEM. (*B*) Course of active EAE in WT and $CCR4^{-/-}$ mice (n = 8–11 mice per group; $P < 0.001$, days 12–22; $P < 0.05$, days 24–26). (*C*) Immunohistochemistry of spinal cord sections from WT and $CCR4^{-/-}$ mice (n = 8 mice per group). (*D*) Flow cytometry of CNS-isolated mononuclear cells of WT and $CCR4^{-/-}$ mice. Representative dot plots show percentages of $CD4^+$ T cells ($CD45^{high}$ pregated) in WT and $CCR4^{-/-}$ mice (mean ± SE; dot blots $P < 0.0001$; n = 12–13 mice per group). (*E*) ELISpot analysis of CNS-isolated IL-17–producing MOG-reactive lymphocytes from MOG-immunized WT and $CCR4^{-/-}$ mice (**$P <$ 0.01). (*F*) EAE in BM chimeric mice after MOG immunization. Lethally irradiated WT mice were reconstituted with WT or $CCR4^{-/-}$ BM cells (n = 8–11 mice per group; $P < 0.001$, days 14–34). (*G*) EAE in BM chimeric mice after MOG immunization. Lethally irradiated WT or $CCR4^{-/-}$ mice were reconstituted with WT BM cells (n = 8–11 mice per group). Data (*A–E*) are representative of at least two independent experiments.

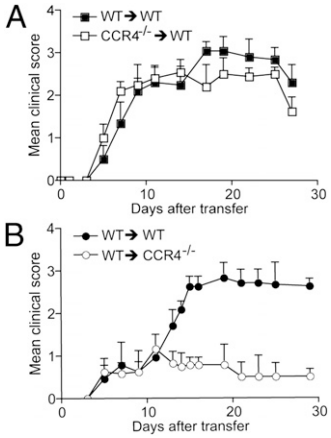

Fig. 2. CCR4$^{-/-}$ mice generate encephalitogenic T cells but are resistant to passive EAE. (*A*) Course of EAE induced in WT mice after adoptive transfer of MOG-reactive WT or CCR4$^{-/-}$ T lymphocytes (n = 5 mice per group). (*B*) Course of EAE in WT and CCR4$^{-/-}$ mice after adoptive transfer of MOG-reactive WT lymphocytes (n = 7 mice per group; $P < 0.01$, days 14–29). Data shown are representative for at least two independent experiments.

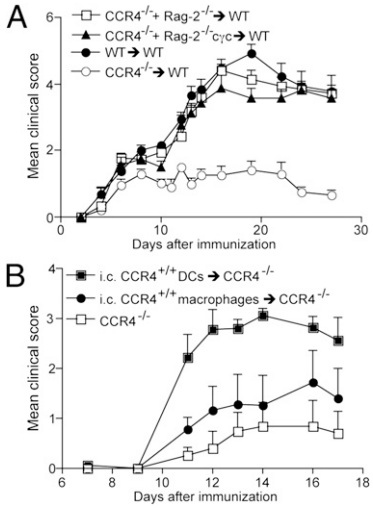

Fig. 3. CCR4-expressing DCs are mediators of EAE. (*A*) Course of EAE in mixed BM chimeric mice. Lethally irradiated WT mice reconstituted with CCR4$^{-/-}$; mixed CCR4$^{-/-}$ and RAG-2$^{-/-}$; mixed CCR4$^{-/-}$ and RAG-2-cγc$^{-/-}$; or WT BM cells (n = 12–13 mice per group) were MOG immunized after 7–8 wk. (*B*) Clinical scores for CCR4$^{-/-}$ mice injected with CCR4$^{+/+}$ MOG DCs or CCR4$^{+/+}$ MOG macrophages and CCR4$^{-/-}$ control mice after MOG immunization (n = 6–8 mice per group). Data shown are representative of at least two independent experiments.

CCR4 expression is not required on T cells, but on another cell type that promotes the inflammatory CNS response during the effector phase of EAE.

Myeloid-Derived CCR4^{+} Cells Are Required for Development of EAE. We generated mixed BM-chimeric mice to test whether CCR4 expression on myeloid cells is required for EAE susceptibility. Thus, lethally irradiated WT mice (CD45.1) were reconstituted with mixed BM from CCR4$^{-/-}$ (CD45.2) and RAG-2$^{-/-}$ (CD45.2) mice (CCR4$^{-/-}$ + RAG-2$^{-/-}$→WT; Fig. S3*A*). In these chimeric mice, all RAG-expressing immune cells were CCR4 deficient, with the exception of APCs and NK cells originating from the RAG-2$^{-/-}$–derived BM cells. As controls, we reconstituted lethally irradiated WT mice either with BM cells from CCR4$^{-/-}$ (CCR4$^{-/-}$→WT) or WT mice (WT→WT). Analysis of peripheral blood lymphocytes (PBL) by flow cytometry revealed equivalent reconstitution efficiency for all mouse groups (Fig. S3*B*). Flow cytometry further detected CCR4 surface expression on CD4^{+} T cells and myeloid-derived cells in the CNS of WT→WT chimeras, but only in RAG-2$^{-/-}$–derived myeloid cells in CCR4$^{-/-}$ + RAG-2$^{-/-}$→WT chimeras (Fig. S3*C*). As seen previously, chimeric WT mice reconstituted with CCR4$^{-/-}$ BM cells (CCR4$^{-/-}$→WT) were resistant to EAE induction (Fig. 3*A*). In striking contrast, mixed BM chimeras (CCR4$^{-/-}$ + RAG-2$^{-/-}$→WT) exhibited a severe clinical manifestation of EAE after MOG immunization with equivalent incidence and severity as observed in controls (WT→WT). These findings indicate that EAE induction requires CCR4 expression on myeloid cells but not on T cells.

In a second set of mixed BM chimeric mice, the contribution of CCR4 expression on APCs vs. NK cells during EAE was investigated. For this, lethally irradiated WT recipients were reconstituted with CCR4$^{-/-}$ BM cells mixed with BM cells from RAG-2 cγc double-knockout mice, which exhibit T-, B-, and NK-cell deficiency (CCR4$^{-/-}$ + RAG-2$^{-/-}$ cγc$^{-/-}$→WT). Thus, in these chimeric mice, only myeloid cells, and not NK cells, express CCR4. As shown in Fig. 3*A*, CCR4$^{-/-}$ + RAG-2$^{-/-}$ cγc$^{-/-}$→WT chimeric mice developed severe clinical EAE comparable to the clinical manifestation exhibited by chimeric mice reconstituted with WT BM or mixed CCR4$^{-/-}$ + RAG-2$^{-/-}$ BM. These findings demonstrate that CCR4 expression on myeloid, but not NK or T, cells is required for disease induction.

CCR4^{+} DCs Are Mediators of EAE. We aimed to precisely define the nature of the myeloid cells required for mediating CCR4-dependent effects in EAE pathogenesis. We found equivalent numbers of mononuclear cells and percentages of CD11b^{+}, CD11c^{+}, or Ly6C^{+} monocytes in the blood of WT or CCR4$^{-/-}$ mice at various disease stages (Fig. S4*A*). We next assessed CCR4 expression on BM-differentiated DCs or macrophages, or Ly6C^{+} monocytes isolated from the blood or BM. Higher CCR4 expression was detected in BM-derived DCs (BMDCs) compared with TLR ligand-stimulated macrophages or Ly6C^{+} cells from the blood or BM, suggesting a predominant role for DCs in CCR4-mediated functions (Fig. S4*B*).

In a next step we used a stereotactic microinjection approach and investigated the capacity of CCR4-competent macrophages or DCs to mediate EAE after intracerebral inoculation. For this, CCR4$^{-/-}$ mice were MOG immunized and 8–9 d later intracerebrally injected with either CCR4$^{+/+}$ DCs or CCR4$^{+/+}$ macrophages. APCs were MOG loaded before intracerebral transfer. Mean clinical EAE scores were not significantly altered between MOG-immunized CCR4$^{-/-}$ controls or CCR4$^{-/-}$ mice injected with CCR4$^{+/+}$ macrophages (Fig. 3*B*). In striking contrast, CCR4$^{-/-}$ mice developed an aggravated clinical manifestation of EAE with tail and hind paralysis if they were i.c. injected with CCR4$^{+/+}$ DCs ($P < 0.01$, days 11–17; for i.c. CCR4$^{+/+}$ DCs → CCR4$^{-/-}$ mice vs. MOG-immunized controls). Moreover, the intracerebral inoculation using CCR4$^{-/-}$ DCs did not lead to a significant altered EAE course in CCR4$^{-/-}$ mice (Fig. S4*C*). These findings demonstrate that CCR4-expressing DCs but not macrophages are required for EAE development, and further suggest that an inherent defect in CCR4$^{-/-}$ DCs in providing the required milieu in the CNS for pathogenic T cells is the prevalent mechanism for EAE resistance in CCR4$^{-/-}$ mice.

CCR4$^{-/-}$ DCs Are Capable in Maturation, T-Cell Priming, and in Vivo Migration. We next tested CCR4$^{-/-}$ DCs for their capacity to induce naive T cells. CCR4$^{-/-}$ and WT BMDCs exhibited similar expression levels of MHC class II, CD40, CD80, and CD86 upon TLR ligand stimulation (Fig. S5*A*). In addition, MOG-loaded splenic WT or CCR4$^{-/-}$ DCs cultured with 2D2 T cells expressing a transgenic MOG-specific TCR (27) induced an equivalent proliferation in these cells (Fig. S5*B*). Furthermore, MOG-reactive WT or CCR4$^{-/-}$ CD4^{+} T cells exhibited equivalent percentages of IFN-γ– and IL-17–secreting cells, independent of whether they were rechallenged for 3 d with MOG-loaded CCR4$^{-/-}$ or WT BMDCs (Fig. S5*C*). Overall, these experiments revealed no differences between CCR4$^{-/-}$ and WT DCs in priming of naïve T cells.

To evaluate the influence of CCR4 on DC migration in vivo, competitive transfer assays were performed. Fluorescently labeled CCR4$^{-/-}$ BMDCs (carboxyfluorescein succinimidyl ester positive, CD45.2) were s.c. coinjected with BMDCs from C57BL/6 (CD45.1) mice in a 1:1 ratio into RAG-2$^{-/-}$ (CD45.2) recipients. CCR4$^{-/-}$ and C57BL/6 DCs were selectively detected in the draining lymph node (LN) in approximately equal percentages by flow cytometry after 48 h and not found in the nondraining LN, suggesting that CCR4$^{-/-}$ DCs were capable of migrating from the peripheral tissue to the local LN (Fig. S5*D*). Furthermore, equal numbers of immigrating CD45^{high} DCs were present in the CNS of CCR4$^{-/-}$ mice compared with WT controls at day 10 after active immunization. This finding suggests that there is no major difference in CNS migration in CCR4$^{-/-}$ mice at the onset of disease (Fig. S5*E*). Overall, these experiments revealed no functional deficits of CCR4$^{-/-}$ DCs in vitro or a reduced migratory capacity compared with WT DCs in vivo.

Reduced IL-23 Production and Maintenance of T_H-17 Cells by CCR4$^{-/-}$ DCs. We next examined the ability of DCs from WT vs. CCR4$^{-/-}$ mice to produce cytokines implicated in EAE pathogenesis (28, 29). BMDCs from WT vs. CCR4$^{-/-}$ mice produced similar levels of TNF, IL-6, and IL-12 after TLR ligand stimulation (Fig. S6*A*). However, BMDCs produced significantly less IL-23 in the absence of CCR4 (Fig. 4*A* and Fig. S6*A*). IL-23 was critically implicated in EAE development before by promoting T_H-17 cells responses (30–32). To examine the capability of CCR4$^{-/-}$ DCs to maintain T_H-17 cells in vitro, purified CD4$^+$ WT T cells from MOG-immunized mice were cocultured with MOG-loaded CCR4$^{-/-}$ DCs or WT DCs. Equivalent percentages of T_H-17 cells in MOG-reactive CD4 T cells were induced when rechallenged with MOG-loaded WT or CCR4$^{-/-}$ DCs from day 1 to day 3 (Fig. S6*B*). Though on day 4, percentages of IFN-γ– or IFN-γ/IL-17–producing CD4$^+$ T cells were equal in these cultures, percentages of T_H-17 cells were significantly reduced in the cultures with CCR4$^{-/-}$ DCs but not WT DCs or phorbol 12-myristate 13-acetate (PMA) ionomycin (Fig. 4*B* and Fig. S6*C*). These results indicated that CCR4$^{-/-}$ DCs display a defect in IL-23 production and concomitantly are less efficient in the maintenance of T_H-17 responses.

Next, IL-23 expression was investigated in the CNS of WT and CCR4$^{-/-}$ mice at peak disease by ELISA, and revealed significant reduced cytokine levels in the CCR4$^{-/-}$ CNS (Fig. 4*C*). IL-23 release was also reduced in CNS-immigrating DCs in the CCR4$^{-/-}$ CNS compared with WT controls, as verified by intracellular cytokine staining of CNS mononuclear cells isolated at this time point (Fig. 4*D*).

To assess whether IL-23 production was required in DCs, we intracerebrally inoculated MOG-immunized CCR4$^{-/-}$ mice with IL-23$^{-/-}$ DCs (Fig. 4*E*). CCR4$^{-/-}$ injected with IL-23$^{-/-}$ DCs showed a milder clinical manifestation of EAE and recovered significantly earlier than CCR4$^{-/-}$ controls injected with CCR4$^{+/+}$ DCs ($P < 0.05$, days 17–23; $P < 0.01$, day 25 for i.c. IL-23$^{-/-}$ DCs→CCR4$^{-/-}$ mice vs. CCR4$^{+/+}$ DCs→CCR4$^{-/-}$ controls).

Finally, the requirement of IL-23 for EAE pathogenesis was investigated in CCR4$^{-/-}$ mice. We found that the i.c. injection of IL-23 fully reverted the EAE-resistant state in MOG-immunized CCR4$^{-/-}$ mice, because the reconstitution with 500 ng IL-23 (but not 75 ng) induced severe disease in these mice (Fig. 4*F*). Even CCR4$^{-/-}$ mice injected with IL-23 intraventricularily or intraspinally—the latter an area where lesions would preferentially develop during MOG-EAE—developed an aggravated clinical form of disease (Fig. S6*D*). Our findings thus suggest that IL-23 produced by DCs modulates EAE development in this model.

CCR4 Ligands Induce IL-23 Release in CCR4$^+$ DCs via a GM-CSF–Dependent Pathway. We asked whether CCR4 ligands regulate IL-23 production in DCs. DCs treated with CCL17/22 in vitro did not exhibit altered IL-23 production, demonstrating that these CCR4 ligands are not able to directly induce IL-23 release in DCs (29.8 ± 0.3 vs. 28.7 ± 0.8 pg/mL; or 29.7 ± 0.3 vs. 27.7 ± 0.3 pg/mL unstimulated vs. CCL17/22 stimulated WT or CCR4$^{-/-}$ DCs, respectively). Next, we evaluated whether the CCR4-CCL17/CCL22 axis promotes IL-23 production by acting on upstream factors known previously to trigger IL-23 release in DCs, such as GM-CSF (33). Indeed, treatment of DCs with CCL17/CCL22 led to GM-CSF production in CCR4-competent DCs, but not in CCR4$^{-/-}$ DCs in vitro (Fig. 5*A*).

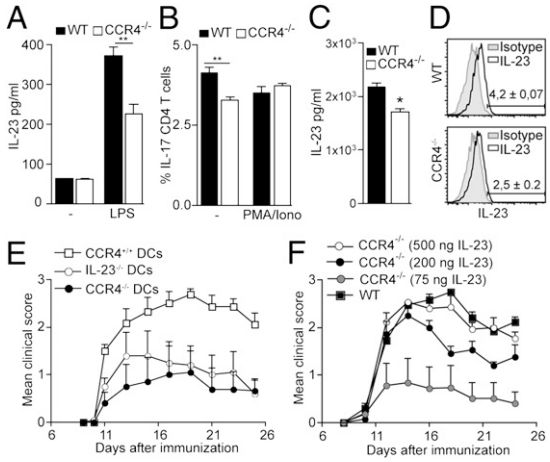

Fig. 4. Reduced IL-23 production and maintenance of T_H-17 cells in CCR4$^{-/-}$ DCs. (*A*) ELISA of IL-23 production in WT or CCR4$^{-/-}$ BMDCs after stimulation with TLR ligands. Shown are mean ± SEM of cytokine levels in culture supernatants; n = 8 mice per group. (*B*) Percentages of IL-17–producing MOG-reactive CD4$^+$ T cells after in vitro rechallenge with MOG-loaded WT DCs or CCR4$^{-/-}$ DCs or PMA/ionomycin. Diagram shows mean IL-17–producing cells ± SE; n = 4–5 MOG-immunized mice per group. (*C*) ELISA of IL-23 in the WT and CCR4$^{-/-}$ CNS at peak of disease. Mean protein amount per CNS ± SEM; n = 3–4 mice per group. (*D*) Flow cytometry of IL-23–producing CNS invading DCs of MOG-immunized WT and CCR4$^{-/-}$ mice at peak disease. Representative histograms show percentages of IL-23–producing DCs (CD45^{high} CD11c$^+$ pregated) in the WT or CCR4$^{-/-}$ CNS. Mean ± SEM; n = 5–6 mice per group; $P < 0.01$. (*E*) Clinical scores for CCR4$^{-/-}$ mice injected i.c. with IL-23$^{-/-}$ MOG-loaded DCs, CCR4$^{+/+}$ MOG-loaded DCs, or CCR4$^{-/-}$ MOG-loaded DCs (n = 5–6 mice per group). (*F*) Clinical scores for CCR4$^{-/-}$ mice injected i.c. with IL-23 (days 8–9 after MOG immunization) or MOG-immunized WT controls (n = 6–8 mice per group; $P < 0.05$, days 14; $P < 0.01$, days 16–24; for i.c. 75 ng IL-23 CCR4$^{-/-}$ vs. WT mice). Data are representative of at least two independent experiments; $^{**}P < 0.01$; $^{*}P < 0.05$.

GM-CSF levels were significantly reduced in the CCR4$^{-/-}$ CNS compared with WT controls at the peak of disease (Fig. 5*B*). In addition, GM-CSF production was not detected by flow cytometry in immigrating DCs in the CCR4$^{-/-}$ CNS in contrast to WT controls (Fig. 5*C*). Also, levels of GM-CSF produced by mononuclear cells isolated from the CCR4$^{-/-}$ CNS were significantly lower than those released from WT cells (Fig. 5*D*). Furthermore, increasing the concentrations of GM-CSF in the DC cultures resulted in a dose-dependent increase in IL-23 production in LPS-stimulated CCR4-competent but not in CCR4-deficient DCs (Fig. 5*E*). Accordingly, GM-CSF$^{-/-}$ DCs produced significantly lower levels of IL-23 compared with C57BL/6 controls, indicating that cell-autonomous processes are involved in GM-CSF–dependent IL-23 production in DCs (Fig. 5*F*). To analyze if the reduced responsiveness of CCR4$^{-/-}$ DCs toward GM-CSF stimulation was the result of a reduced presence of the receptor for GM-CSF on these cells, we analyzed mRNA or protein surface expression of csfr2b in CCR4$^{-/-}$ DCs vs. WT DCs (Fig. S7). mRNA expression and surface protein of csfr2b was present in equal amounts in CCR4$^{-/-}$ DCs vs. WT DCs, suggesting that intracellular signal transduction pathways downstream of csfr2b may be modified in CCR4$^{-/-}$ DCs (Fig. S7). We also found that production of IL-23 was significantly reduced in LPS-stimulated C57BL/6 DCs after blocking endogenous CCL17/22 with anti-CCL17/22 antibodies (Fig. 5*F*). This finding indicates an additional cell-autonomous mode of how DCs modulate IL-23 secretion. In summary, these data demonstrate that production of IL-23 in DCs is CCR4 dependent and

regulated via an indirect GM-CSF–dependent manner through CCL17 and CCL22.

Finally we asked whether GM-CSF production was required in DCs for EAE development, and used GM-CSF$^{-/-}$ DCs for intracerebral inoculation in this model. As shown in Fig. 5*G*, GM-CSF$^{-/-}$ DCs failed to induce EAE in CCR4$^{-/-}$ mice. Together, these findings suggest that CCR4-expressing DCs are critical for the development of EAE via GM-CSF–dependent IL-23 production in these cells.

Discussion

In this study we identified DCs as the relevant cell type mediating CCR4-dependent effects in the development of EAE. Our results demonstrated that CCR4$^{-/-}$ mice not only exhibited an attenuated clinical course of EAE upon MOG immunization, but were also resistant to EAE induction following transfer of encephalitogenic WT lymphocytes. The expression of CCR4 only in myeloid-derived cells in a BM-chimeric model and the intracerebral injection of CCR4^{+} DCs was required for EAE development and defined CCR4^{+} DCs as key mediators of EAE in this model. We showed that CCR4$^{-/-}$ DCs displayed a defect in the GM-CSF–dependent production of IL-23, and that both cytokines are required to be secreted by DCs for development of EAE in this model.

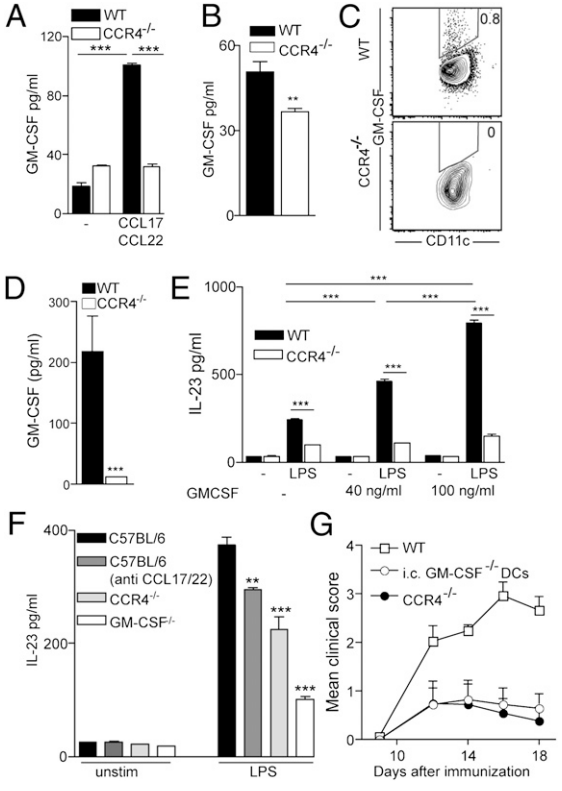

Fig. 5. CCR4 ligands induce IL-23 release in CCR4^{+} DCs via a GM-CSF–dependent pathway. (*A*) GM-CSF release in BMDCs from WT or CCR4$^{-/-}$ mice after CCL17/CCL22 stimulation (n = 5 mice per group; mean protein amount ± SEM). (*B*) GM-CSF levels in the CNS of WT and CCR4$^{-/-}$ mice at peak of disease. Mean protein amount/CNS ± SEM; n = 3–4 mice per group. (*C*) Representative dot plots of GM-CSF production in CD45^{high} CNS-invading DCs in WT and CCR4$^{-/-}$ mice. (*D*) ELISA of GM-CSF produced by CNS mononuclear cells of WT and CCR4$^{-/-}$ mice after LPS stimulation. Mean protein amount ± SEM; n = 5–6 mice per group. (*E*) IL-23 release by WT or CCR4$^{-/-}$ BMDCs after LPS stimulation without or with GM-CSF. Mean protein amount ± SEM; n = 5 mice per group; ***P < 0,001. (*F*) IL-23 release by C57BL/6; C57BL/6 treated with anti-CCL17/22; CCR4$^{-/-}$; and GM-CSF$^{-/-}$ DCs with or without LPS. Mean protein amount ± SEM; n = 4–5 mice per group. **P < 0.01, ***P < 0,001 between indicated group compared with C57BL/6 DCs. (*G*) Clinical scores for CCR4$^{-/-}$ mice i.c. injected with GM-CSF$^{-/-}$ DCs or MOG-immunized WT or CCR4$^{-/-}$ mice (n = 7–8 mice per group; P < 0.05, day 12; P < 0.01, day 14; P < 0.001, days 16–18). Data are representative of at least two independent experiments.

To date, only a few studies have characterized myeloid cell-expressed CCRs as susceptibility factors associated with EAE. In this regard, CCR2 has been shown to affect EAE pathogenesis based on observations that CCR2$^{-/-}$ mice were resistant to EAE, although this effect was dependent on the genetic background of the mice (34–36). Recent studies have unraveled the mechanism of disease resistance in CCR2$^{-/-}$ animals by demonstrating a disease-promoting role of CCR2^{+} Ly-6C^{high} monocytes during induction of EAE (37). During the preparation of this manuscript, it was further suggested that a reduction in the numbers of (TNF-producing) inflammatory macrophages observed in CNS, spleen, and LN were causative for enhanced EAE resistance in CCR4$^{-/-}$ mice (38). Our data, however, indicate that equal numbers of myeloid cells (including inflammatory macrophages) are present in the peripheral blood of WT or CCR4$^{-/-}$ mice at various disease stages. In accordance with this previous study we identified reduced numbers of CNS-immigrating myeloid cells in CCR4$^{-/-}$ mice at peak disease. Also, CCR4 expression in myeloid cells but not in lymphocytes was shown to be critical in EAE development. Here we demonstrate a functional role for CCR4 expressed by DCs, but not by macrophages, in mediating EAE pathogenesis. Highest CCR4 mRNA expression in DCs suggested these myeloid cells as promising candidates that mediate CCR4 effects in EAE development. The fact that intracerebral reconstitution using CCR4^{+} DCs (but not CCR4^{+} macrophages) induced EAE in CCR4$^{-/-}$ mice defined these cells as relevant in CCR4-mediated development of CNS autoimmunity.

Earlier studies showed that the presence and function of DCs in the CNS correlates with EAE severity (6, 8). These professional APCs have been suggested to participate in restimulation of myelin-specific CD4^{+} T cells in the CNS (5, 7, 39, 40). The identification of equal numbers of DCs in the CCR4$^{-/-}$ and WT CNS at the onset of disease suggested no major differences in CNS migration, but cannot fully exclude that migratory deficits of CCR4$^{-/-}$ DCs occur at a later time point during disease development. However, we could not detect a defect in basic DC functions in CCR4$^{-/-}$ DCs, e.g., migration from peripheral sites, expression of costimulator molecules, and antigen presentation. The fact that functional encephalitogenic T cells were induced in CCR4$^{-/-}$ mice further demonstrates the capacity of CCR4$^{-/-}$ DCs in activating naive T cells.

Importantly, we could demonstrate that CCR4$^{-/-}$ DCs were deficient in IL-23 production and maintaining (long-term) T_H-17 cell cultures. We further showed that CCR4 regulated IL-23 production in DCs via an indirect mode. CCL17/CCL22 up-regulated CCR4-dependent production of GM-CSF in DCs, which in turn induced IL-23 secretion in CCR4^{+} DCs in an auto or paracrine manner. The relevance of the IL-23/IL-17 axis in the pathogenesis of CNS autoimmunity is well established. For example, p19-deficient mice (one of the heterodimeric IL-23 subunits) failed to develop EAE after MOG immunization (30, 31). The critical role of IL-23 in mediating EAE pathology was ascribed to its ability to cause an accumulation of myelin-specific T_H-17 cells in the CNS rather than expanding autoreactive cells in the periphery (32). Recent studies have further defined the impact of GM-CSF in this process because it can act to stimulate DC production of IL-23 during autoimmune responses. However, GM-CSF–mediated effects on IL-23 production by DCs have been attributed before to T cells (33). Two recent studies demonstrated that T-cell–derived GM-CSF sustained neuroinflammation via myeloid cells that infiltrated the CNS (41, 42). Our studies now extend these data and define that GM-CSF production in DCs is regulated by CCR4 and is required for the development of EAE through modulation of IL-23. The findings that GM-CSF$^{-/-}$ DCs produced significantly lower levels of IL-23 compared with C57BL/6 controls provide further evidence that IL-23 production in DCs is also propagated by a GM-CSF–dependent autocrine mechanism. We further showed that CCR4$^{-/-}$ mice exhibited (*i*) reduced GM-CSF and IL-23 protein levels in the CNS and (*ii*) a defect in GM-CSF and IL-23 production in CNS-immigrating

IMMUNOLOGY

DCs after MOG immunization. The intraspinal reconstitution with IL-23 induced development of EAE in CCR4$^{-/-}$ mice.

DC-derived IL-23 or GM-CSF were further shown to be major components in disease progression, because the intracerebral inoculation using IL-23$^{-/-}$ or GM-CSF$^{-/-}$ DCs failed to induced EAE in CCR4$^{-/-}$ mice in contrast to WT DCs. Of note, exogenously added CCL17/22 induced the production of only small amounts of GM-CSF, even by CCR4^{+} DCs in in vitro cultures, whereas high levels of exogenous GM-CSF significantly enhanced IL-23 production by DCs. This finding suggests that other cells (e.g., monocytes) contribute to IL-23 production by DCs in this model; however, the small amounts of GM-CSF produced by DCs are absolutely required for EAE development.

Our findings suggest that CCR4-mediated signals confer a positive feedback loop during the development of EAE. That is, myeloid cells (like DCs or macrophages) expressing CCR4 receptors are also capable of producing CCL17 and CCL22, thereby perpetuating myeloid cell infiltration (16, 22). Furthermore, this study identified CCR4^{+} DCs as key cellular components required for the initiation of the recruitment process. Defective production of CCR4 ligands by macrophages and DCs in the absence of CCR4 could alternatively cause reduced bystander recruitment, leading to diminished numbers of local encephalitogenic T cells and, in consequence, reduced numbers of macrophages and DCs. Recently, Dogan et al. (43) showed that CCL22 played a regulatory role in EAE by mediating inflammatory macrophage accumulation in the CNS and affecting effector functions. Consistent with this hypothesis, a defect in CCL22 production by CCR4$^{-/-}$ APCs was found following stimulation with TLR ligands (26). The increased numbers of myeloid cells in the CNS might represent the critical mass needed for the generation of the appropriate cytokines and chemokines (including GM-CSF–mediated regulation of IL-23 in DCs) required for the maintenance of encephalitogenic T cells in the CNS.

In summary, our findings show an essential role for CCR4 expressed by DCs for EAE pathogenesis. Therefore, targeting DC-specific CCR4 signaling pathways is a promising therapeutic approach to the treatment of CNS autoimmunity.

Materials and Methods

Active EAE Induction. Active EAE induction by tail-base immunization of mice with 50 μg of $MOG_{35–55}$ (Biotrend) in CFA, supplemented with 10 mg/mL *Mycobacterium tuberculosis* H37RA (Difco Laboratories) and i.p. injection of 200 ng pertussis toxin on days 0 and 2.

Generation of BM Chimeric Mice. A total of 9.5 Gy-irradiated mice were i.v. reconstituted with 0.8–1.2 × 10^7 BM cells. Mixed BM chimeras were reconstituted with 0.2–0.4 × 10^7 BM cells (RAG-2$^{-/-}$ or RAG-2$^{-/-}$cγc$^{-/-}$) mixed with 0.8–1.0 × 10^7 CCR4$^{-/-}$ BM cells. Additional information is available in *SI Materials and Methods*.

ACKNOWLEDGMENTS. We thank R. M. Ransohoff, C. Kurts, T. Buch, F. Kurschus, and S. Specht for discussion; J. Buer, H. Jonuleit, L. Diehl, F. Kurschus, L. Codarri, and B. Becher for mouse strains; and H. Schrage, F. Frommer, and M. Herold for excellent experimental help. This work was supported by the Deutsche Forschungsgemeinschaft (FOR 926, KA 2306/1-1) and the German Federal Ministry of Education and Research Grant NGFN Plus; FKZ: 01GS08144.

1. Lassmann H (2008) Models of multiple sclerosis: New insights into pathophysiology and repair. *Curr Opin Neurol* 21:242–247.
2. Steinman L, Zamvil SS (2006) How to successfully apply animal studies in experimental allergic encephalomyelitis to research on multiple sclerosis. *Ann Neurol* 60:12–21.
3. Wekerle H (2008) Lessons from multiple sclerosis: Models, concepts, observations. *Ann Rheum Dis* 67(Suppl 3):iii56–iii60.
4. Segal BM (2003) Experimental autoimmune encephalomyelitis: Cytokines, effector T cells, and antigen-presenting cells in a prototypical Th1-mediated autoimmune disease. *Curr Allergy Asthma Rep* 3:86–93.
5. Miller SD, McMahon EJ, Schreiner B, Bailey SL (2007) Antigen presentation in the CNS by myeloid dendritic cells drives progression of relapsing experimental autoimmune encephalomyelitis. *Ann N Y Acad Sci* 1103:179–191.
6. Greter M, et al. (2005) Dendritic cells permit immune invasion of the CNS in an animal model of multiple sclerosis. *Nat Med* 11:328–334.
7. McMahon EJ, Bailey SL, Miller SD (2006) CNS dendritic cells: Critical participants in CNS inflammation? *Neurochem Int* 49:195–203.
8. Zozulya AL, et al. (2009) Intracerebral dendritic cells critically modulate encephalitogenic versus regulatory immune responses in the CNS. *J Neurosci* 29:140–152.
9. Ransohoff RM (2009) Chemokines and chemokine receptors: Standing at the crossroads of immunobiology and neurobiology. *Immunity* 31:711–721.
10. Sallusto F, Baggiolini M (2008) Chemokines and leukocyte traffic. *Nat Immunol* 9:949–952.
11. Chvatchko Y, et al. (2000) A key role for CC chemokine receptor 4 in lipopolysaccharide-induced endotoxic shock. *J Exp Med* 191:1755–1764.
12. Yuan Q, et al. (2007) CCR4-dependent regulatory T cell function in inflammatory bowel disease. *J Exp Med* 204:1327–1334.
13. Berahovich RD, Lai NL, Wei Z, Lanier LL, Schall TJ (2006) Evidence for NK cell subsets based on chemokine receptor expression. *J Immunol* 177:7833–7840.
14. Romagnani S (2002) Cytokines and chemoattractants in allergic inflammation. *Mol Immunol* 38:881–885.
15. Stutte S, et al. (2010) Requirement of CCL17 for CCR7- and CXCR4-dependent migration of cutaneous dendritic cells. *Proc Natl Acad Sci USA* 107:8736–8741.
16. Alferink J, et al. (2003) Compartmentalized production of CCL17 in vivo: Strong inducibility in peripheral dendritic cells contrasts selective absence from the spleen. *J Exp Med* 197:585–599.
17. Yamashita U, Kuroda E (2002) Regulation of macrophage-derived chemokine (MDC, CCL22) production. *Crit Rev Immunol* 22:105–114.
18. Franciotta D, et al. (2006) Cytokines and chemokines in cerebrospinal fluid and serum of adult patients with acute disseminated encephalomyelitis. *J Neurol Sci* 247: 202–207.
19. Narikawa K, et al. (2004) CSF chemokine levels in relapsing neuromyelitis optica and multiple sclerosis. *J Neuroimmunol* 149:182–186.
20. Galimberti D, et al. (2008) MDC/CCL22 intrathecal levels in patients with multiple sclerosis. *Mult Scler* 14:547–549.
21. Butti E, et al. (2008) IL4 gene delivery to the CNS recruits regulatory T cells and induces clinical recovery in mouse models of multiple sclerosis. *Gene Ther* 15:504–515.
22. Columba-Cabezas S, et al. (2002) Induction of macrophage-derived chemokine/CCL22 expression in experimental autoimmune encephalomyelitis and cultured microglia: Implications for disease regulation. *J Neuroimmunol* 130:10–21.
23. Wu M, Fang H, Hwang ST (2001) Cutting edge: CCR4 mediates antigen-primed T cell binding to activated dendritic cells. *J Immunol* 167:4791–4795.
24. Henry CJ, Ornelles DA, Mitchell LM, Brzoza-Lewis KL, Hiltbold EM (2008) IL-12 produced by dendritic cells augments CD8+ T cell activation through the production of the chemokines CCL1 and CCL17. *J Immunol* 181:8576–8584.
25. Semmling V, et al. (2010) Alternative cross-priming through CCL17-CCR4-mediated attraction of CTLs toward NKT cell-licensed DCs. *Nat Immunol* 11:313–320.
26. Ishii M, et al. (2008) CC chemokine receptor 4 modulates Toll-like receptor 9-mediated innate immunity and signaling. *Eur J Immunol* 38:2290–2302.
27. Bettelli E, et al. (2003) Myelin oligodendrocyte glycoprotein-specific T cell receptor transgenic mice develop spontaneous autoimmune optic neuritis. *J Exp Med* 197: 1073–1081.
28. Segal BM (2010) Th17 cells in autoimmune demyelinating disease. *Semin Immunopathol* 32:71–77.
29. El-behi M, Rostami A, Ciric B (2010) Current views on the roles of Th1 and Th17 cells in experimental autoimmune encephalomyelitis. *J Neuroimmune Pharmacol* 5:189–197.
30. Cua DJ, et al. (2003) Interleukin-23 rather than interleukin-12 is the critical cytokine for autoimmune inflammation of the brain. *Nature* 421:744–748.
31. Langrish CL, et al. (2005) IL-23 drives a pathogenic T cell population that induces autoimmune inflammation. *J Exp Med* 201:233–240.
32. Gyülvészi G, Haak S, Becher B (2009) IL-23-driven encephalo-tropism and Th17 polarization during CNS-inflammation in vivo. *Eur J Immunol* 39:1864–1869.
33. Sonderegger I, et al. (2008) GM-CSF mediates autoimmunity by enhancing IL-6-dependent Th17 cell development and survival. *J Exp Med* 205:2281–2294.
34. Gaupp S, Pitt D, Kuziel WA, Cannella B, Raine CS (2003) Experimental autoimmune encephalomyelitis (EAE) in CCR2(–/–) mice: Susceptibility in multiple strains. *Am J Pathol* 162:139–150.
35. Mahad DJ, Ransohoff RM (2003) The role of MCP-1 (CCL2) and CCR2 in multiple sclerosis and experimental autoimmune encephalomyelitis (EAE). *Semin Immunol* 15:23–32.
36. Izikson L, Klein RS, Luster AD, Weiner HL (2002) Targeting monocyte recruitment in CNS autoimmune disease. *Clin Immunol* 103:125–131.
37. Mildner A, et al. (2009) CCR2+Ly-6Chi monocytes are crucial for the effector phase of autoimmunity in the central nervous system. *Brain* 132:2487–2500.
38. Forde EA, Dogan RN, Karpus WJ (2011) CCR4 contributes to the pathogenesis of experimental autoimmune encephalomyelitis by regulating inflammatory macrophage function. *J Neuroimmunol* 236:17–26.
39. Serafini B, et al. (2006) Dendritic cells in multiple sclerosis lesions: Maturation stage, myelin uptake, and interaction with proliferating T cells. *J Neuropathol Exp Neurol* 65:124–141.
40. Pashenkov M, et al. (2001) Two subsets of dendritic cells are present in human cerebrospinal fluid. *Brain* 124:480–492.
41. Codarri L, et al. (2011) RORγt drives production of the cytokine GM-CSF in helper T cells, which is essential for the effector phase of autoimmune neuroinflammation. *Nat Immunol* 12:560–567.
42. El-Behi M, et al. (2011) The encephalitogenicity of T(H)17 cells is dependent on IL-1- and IL-23-induced production of the cytokine GM-CSF. *Nat Immunol* 12:568–575.
43. Dogan RN, et al. (2011) CCL22 regulates experimental autoimmune encephalomyelitis by controlling inflammatory macrophage accumulation and effector function. *J Leukoc Biol* 89:93–104.

Supporting Information

Poppensieker et al. 10.1073/pnas.1114153109

SI Materials and Methods

Mice. C57BL/6 (H-2^b) female mice were purchased from Janvier or bred locally. CC chemokine receptor 4 (CCR4)-deficient ($CCR4^{-/-}$, N10 backcross to C57BL/6), CD45.1, and RAG-$2^{-/-}$ mice were purchased from the Jackson Laboratory. RAG-2/cγc double-knockout mice were kindly provided by Jan Buer (University Hospital Essen, Essen, Germany) and Helmut Jonuleit (University of Mainz, Mainz, Germany). GM-CSF knockout mice were kindly provided by Laura Codarri and Burkhard Becher (University of Zurich, Zurich). All animals were bred and housed in the specific pathogen-free animal facility of the House for Experimental Therapy (University of Bonn) according to German guidelines for animal care. Ethical approval for the use of all mice in this study was obtained from the German government.

Passive Experimental Autoimmune Encephalomyelitis Induction. Passive experimental autoimmune encephalomyelitis (EAE) was induced by immunizing female mice (8–10 wk) s.c. with 100 μg of myelin oligodendrocyte glycoprotein peptide p35–55 ($MOG_{35–55}$) in complete Freund's adjuvant containing 10 mg/mL *Mycobacterium tuberculosis* H37Ra. Spleens were harvested 10 d later and prepared as single-cell suspensions, then cultured in RPMI 1640 complete medium with 10% FCS, penicillin/streptomycin, L-glutamine, nonessential amino acids, 2-ME (Invitrogen Life Technologies), restimulated $MOG_{35–55}$ (20 μg/mL), and recombinant murine IL-12 (20 ng/mL; R&D Systems) or PBS. After 3 d, cells were harvested and $1.5–2 \times 10^7$ cells were transferred i.p. into recipient mice. Recipient mice were given 200 ng of pertussis toxin i.p. on day 0 and day 2 posttransfer. EAE scores as follows: 0, no clinical signs; 1, loss of tail tonicity; 2, loss of tail tonicity and hindlimb paresis; 3, loss of tail tonicity and hindlimb paralysis; 4, hindlimb and forelimb paresis; 5, hindlimb and forelimb paralysis; 6, moribund/death.

CNS Mononuclear Cell Isolation. At various stages of disease, mice were anesthetized, perfused with 20 mL of ice cold PBS. Brain and spinal cord tissue samples were collected and homogenized by two steps of digestion with collagenase/dispase (Roche) and DNase I (Roche) at 37 °C for 45 min each, and mononuclear cells were isolated using Percoll gradients. Mononuclear cells were collected from the 30%/70% interface of a Percoll gradient after centrifugation at $922 \times g$ for 25 min at room temperature. Following collection, cells were stored on ice for further use.

Flow Cytometry and Cell Sorting. Fluorescence staining of cell samples was performed using the following: FITC-, phycoerythrin-, Allophycocyanine (APC)-, or Alexa 647-labeled or biotinylated antibodies or secondary reagents (SA-PerCP-Cy5.5; all purchased from BD Biosciences): anti-mCD4; anti-mCD45.1; anti-mCD45.2; anti-mCD11c; anti-mCD11b; anti-mTCRβ; anti-B220; anti-I-A/E^b; anti-mCD8α; anti-IFN-γ; anti-IL-17; anti-Ly6C and anti-IL-12 p40; goat anti-mCCR4 antibody (Abcam) or anti-mCCR4 (eBiosciences); and FITC- or Alexa 647-conjugated donkey anti-goat IgG (Jackson ImmunoResearch). Anti-CD131 antibody was kindly provided by Tobias Suter (University Hospital of Zurich, Zurich). CCR4 staining required immediate fixation of cells after staining procedure as used for cytokine staining according to the manufacturer's instructions (BD Biosciences). Fc receptors were blocked with antibodies against mCD16/CD32. Intracellular cytokine staining was performed according to the manufacturer's instructions (BD Biosciences). Samples were acquired using a Canto II flow cytometer and acquired data analyzed using FlowJo (TreeStar). Sorting of $CD11b^+$, $CD45^{high}$, and $CD45^{low}$ cells or $CD4^+$ T cells out of CNS isolated mononuclear cells was performed on a BD FACSAria. The purity of the sorted cell populations was >95%. In some experiments (flow cytometry for CCR4 expression), $CD4^+$ T cells or $CD11b^+$ cells were enriched to >98% purity after isolation from the CNS by MACS (Miltenyi Biotec) using anti-CD4 or anti-CD11b-conjugated microbeads. $Ly6C^+$ cells were enriched to >98% purity after isolation from the bone marrow (BM) and from peripheral blood isolated lymphocytes by streptavidin-conjugated MACS (Miltenyi Biotec) using biotinylated anti–Ly6C-conjugated microbeads.

Cytokines/Chemokines. Recombinant murine CCL17 and CCL22 were obtained from R&D Systems and used in the cultures at a final concentration of 250 ng/mL. Mouse IL-12 was used at a concentration of 20 ng/mL.

Generation and in Vitro Stimulation of BM Dendritic Cells, BM Macrophages, and CNS Isolated Mononuclear Cells. Bone marrow dendritic cells (BMDCs) were generated as described previously (1). In some experiments, BMDCs were enriched with anti-CD11c (N418) magnetic microbeads (Miltenyi Biotec). For generation of BM macrophages, BM cells were cultured in 1×10^5 cells/mL in RPMI supplemented with 10% vol/vol heat-inactivated FCS, L-glutamine, penicillin-streptomycin, 2-ME (all GIBCO-BRL), and 30% conditioned medium of L292 cells. On day 3, adherent cells were recultured in complete medium and harvested on day 7. BMDCs were stimulated in vitro for indicated times with 100 ng/mL *Escherichia coli* LPS serotype 0127:B8 (Sigma-Aldrich), unmethylated cytosine-guanosine dinucleotide-containing oligonucleotides (1 μM; TIB MOLBIOL), and polyinosinic:polycytidylic acid (poly I:C; 50 μg/mL; Sigma-Aldrich). In some experiments, CNS-isolated mononuclear cells were cultured for 15 h in the presence of 100 ng/mL *E. coli* LPS serotype 0127:B8 (Sigma-Aldrich) or 15 μg/mL monoclonal rat anti-mouse CCL17 Ab and monoclonal rat anti-mouse CCL22 Ab (R&D Systems).

Cell Culture for T_H-1 and T_H-17 Differentiation. Mouse splenic $CD4^+$ T cells were isolated by immunomagnetic separation using CD4-MACS beads (Miltenyi Biotec) and stimulated with plate-bound 4 μg/mL αCD3 antibody (145-2C11) and 4 μg/mL αCD28 antibody (3751) together with 5 ng/mL TGF-β and 20 ng/mL IL-6 (PeproTech) for T_H-17 differentiation, and with IL-12 (10 ng/mL) for T_H-1 differentiation. In some experiments, MACS-isolated splenic DCs from WT or $CCR4^{-/-}$ mice were cocultured with T cells in the presence of antigen (20 μg/mL MOG).

In Vivo DC Migration and Stereotactic Intracerebral Injection of APCs or mouse IL-23. MACS-enriched BMDCs from $CCR4^{-/-}$ mice (CD45.2) were labeled with the fluorescent dye carboxyfluorescein succinimidyl ester (CFSE; 5 mM) for 15 min at 37 °C before being combined 1:1 with BMDCs from CD45.1 C57BL/6 congenic mice. DCs were injected s.c. into RAG-2 knockout mice and, 48 h later, single-cell suspensions were prepared from the draining and nondraining lymph nodes for analysis by flow cytometry. Stereotactic intracerebral injection was performed as previously described (2). Recipient mice were MOG immunized and i.p. injected with pertussis toxin on day 0 and day 2 after immunization. BMDCs or BM macrophages were loaded with 10 μg of $MOG_{35–55}$/mL before being injected in $CCR4^{-/-}$ mice. On day 8–9

after immunization, experimental mice were placed in a stereotactic frame and received a constant stream of an oxygen/isoflurane mixture to maintain anesthesia. A total of 3–5 × 10^5 MOG-loaded APCs in 10 μL PBS were injected in the left frontal lobe at 0.0 mm (anteroposterior), 2.2 mm (mediolateral), and 1.5 mm (dorsoventral), according to bregma, with a standard insulin syringe attached to a depth controller. For intracerebral delivery of cytokines, recombinant mouse IL-23 (various doses of recombinant mouse IL-23, reconstituted in PBS; R&D Systems) was injected as described for stereotactic intracerebral injection of cells. Intraventricular injections were given via a right lateral ventricular puncture (bregma anteroposterior −0.5 mm, lateral 1 mm, depth 1.8 mm) with a standard insulin syringe attached to a depth controller. For intraspinal injections, mice were anesthetized and placed in a stereotactic frame as described for intracerebral injections. IL-23 was injected into the lumbar spinal cord at the level of the vertebrae thoracicae (TH8-12) following laminectomy. Injections, controlled by an infusion pump, were 0.1 μL/min through a standard insulin syringe with a depth controller. Following injection, the needle was left in place for 5 min before being retrieved.

Histology. For histological analysis, tissues were fixed in 4% buffered formalin fixed and embedded in paraffin as described previously (3). For immunohistochemical analysis of spinal cord tissues, we used monoclonal rat anti-mouse MAC3 (clone M3/84; BD Biosciences), monoclonal rat anti-human/mouse CD3 (clone CD3-12; Serotec), monoclonal rat anti-mouse B220 (clone RA3-6B2; Serotec), and monoclonal mouse anti-amyloid precursor protein (clone 22C11; Chemicon). Secondary reagents included antibody for CD3, MAC3, and B220: biotinylated goat anti-rat Ig (RPN1005); and secondary antibody for APP: sheep anti-mouse Ig (RPN1001; both Amersham Biosciences), using avidin-biotin amplification bridge method with peroxidase as a substrate. In Luxol fast blue staining, total white matter and demyelinated areas from three cross-sections were measured by planimetry, and the area of demyelination was expressed as percent of the total area of the white matter. For each animal, the mean percentage of demyelination of the individual sections was calculated.

Total RNA Preparation. Mouse tissue or cells were rapidly dissected, snap frozen in isopentane, and stored at −80 °C. Total RNA was prepared according to the TRIzol method (Invitrogen). Up to 5 μg RNA and 0.5 μg oligo$(dT)_{20}$ primer (Invitrogen) were heated at 70 °C for 4 min, chilled on ice, then reverse transcribed at 42 °C for 50 min. A total volume of 20 μL included 4 μL first-strand buffer (Invitrogen), 2 μL 0.1 M DTT, 1 μL 10 mM dNTPs, 0.5 μL RNase OUT (Invitrogen), and 200 U SuperScript II reverse transcriptase (Invitrogen).

TaqMan Analysis. RT-quantitative PCR of cDNA samples was performed using an ABI 7900 sequence detector (Perkin-Elmer) and Universal PCR Master Mix (Perkin-Elmer). After incubation of the samples at 50 °C for 2 min and 95 °C for 10 min, 40 cycles of 95 °C for 15 s and 60 °C for 1 min were applied. TaqMan primer and probe sets were ordered from Applied Biosystems as follows: CCR4-Mm 00438271_ml; GAPDH-Mm99999915_gl; Csf2rb-Mm 00655745_ml; b-Actin-Mm00607939_sl. Results are expressed as fold change relative to the control samples normalized to GAPDH.

Chemokine/Cytokine Measurements in Brain Tissue Lysates. For detection of cytokines in brain tissue extracts, brains were removed, stored on ice, homogenized, and lysed using a Precellys homogenater (Precellys; Peqlab) in 1 mL proteinase inhibitor buffer (Roche). The resulting brain homogenate was ultrasonicated for 1 min and centrifuged at 3,000 × *g* for 5 min twice before removing the supernatant and storing it at −80 °C. Cytokines/chemokines in undiluted supernatants of brain lysates were measured using ELISAs according to the manufacturer's instructions (R&D Systems).

Enzyme-Linked Immunosorbent Spot Assay and ELISA. Enzyme-linked immunosorbent spot (ELISpot) assays were used for the detection of cells secreting IFN-γ or IL-17 and were performed according to the manufacturer's instructions (R&D Systems). Briefly, CNS mononuclear cells from MOG-immunized recipients were restimulated by coculturing them at 37 °C, 5% CO_2 for 30 h with MACS-isolated $CD11c^+$ splenic DCs from C57BL/6 mice in the presence of MOG peptide (50 μg/mL) on anti–IL-17A antibody coated or anti-IFN-γ–coated 96-well plates. Afterward, the plates were washed 3× with washing buffer before the plates were developed according to the manufacturer's protocol (R&D Systems). Spots were counted using an automated ELISpot reader (BIOREADER-2000; Biosys). Cytokines in cell culture supernatants were measured using ELISAs according to the manufacturer's instructions (R&D Systems).

Measurement of T-Cell Responses. Splenic T lymphocytes were harvested from WT or $CCR4^{-/-}$ mice MOG immunized 10 d before. Cells were incubated in the presence of BMDCs or splenic DCs generated from WT or $CCR4^{-/-}$ mice and loaded with MOG peptide (50 μg/mL) in RPMI with 10% FCS in 24-well plates (5 × 10^5 cells/mL) for indicated times. Thereafter, intracellular cytokine staining was performed according to the manufacturer's instructions (BD Biosciences). A total of 10 ng/mL phorbol 12-myristate 13-acetate and 1 μg/mL ionomycin (Sigma-Aldrich) were used for stimulation of T cells in cultures.

CFSE Labeling. T cells were enriched to >90% purity from the spleen by MACS (Miltenyi Biotec) using anti–CD4-conjugated microbeads. For proliferation assay, purified $CD4^+$ T lymphocytes were adjusted to 1 × 10^5 cells/mL in prewarmed PBS + 0.1% BSA. A total of 5 mM stock CFSE (Molecular Probes) solution in DMSO was added at 2 μL/mL cells for a final working concentration of 10 μM followed by incubation at 37 °C for 10 min. The staining was quenched by adding (fivefold to cell volume) of ice-cold RPMI 1640 + 10% FCS to the tube. If not indicated otherwise, T-cell proliferation was assessed on day 3 of culture by flow cytometry.

Statistical Analysis. Two-tailed Student *t* tests were used for statistical analyses unless otherwise stated. Mann–Whitney *U* test was used as a nonparametric test when indicated. Results were considered significant if $P < 0.05$. For clinical scores, statistical differences between the experimental groups were evaluated by the repeated-measures ANOVA with Bonferroni's posttest.

1. Alferink J, et al. (2003) Compartmentalized production of CCL17 in vivo: Strong inducibility in peripheral dendritic cells contrasts selective absence from the spleen. *J Exp Med* 197:585–599.
2. Zozulya AL, et al. (2009) Intracerebral dendritic cells critically modulate encephalitogenic versus regulatory immune responses in the CNS. *J Neurosci* 29(1, l):140–152.
3. Mildner A, et al. (2009) $CCR2^+Ly\text{-}6C^{hi}$ monocytes are crucial for the effector phase of autoimmunity in the central nervous system. *Brain* 132:2487–2500.

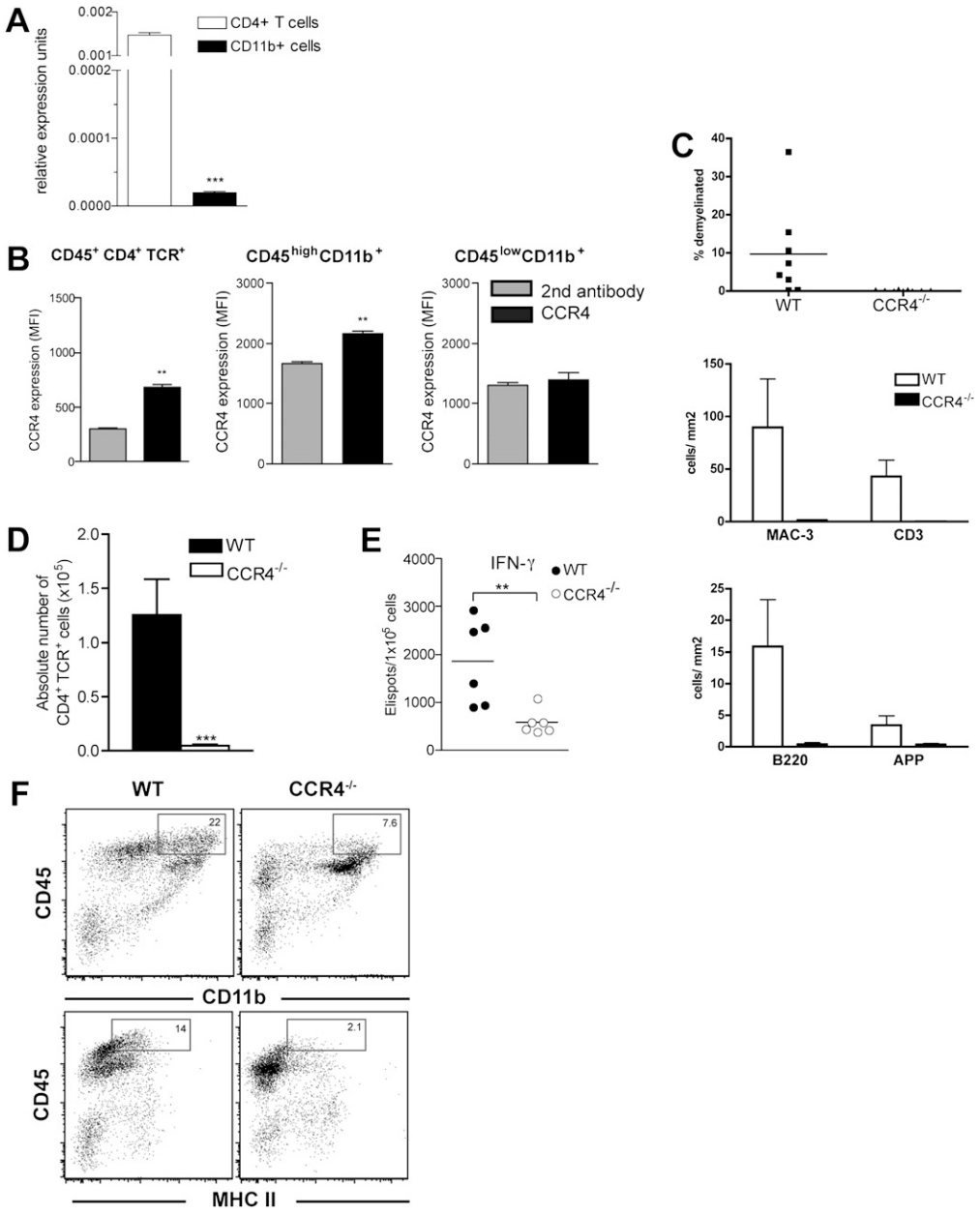

Fig. S1. CCR4 expression during EAE. (*A*) RT-PCR analysis of CCR4 mRNA levels in CNS-isolated $CD4^+$ T cells or $CD11b^+$ cells of C67BL/6 mice at peak disease. mRNA levels are normalized to GAPDH expression and results are presented as mean ± SEM (n = 5 mice; $P < 0.0001$). Data shown are representative of two independent experiments. (*B*) CCR4 surface expression on $CD4^+$ T cells and $CD11b^+$ cells in the CNS of EAE-induced C57BL/6 mice. Shown are diagrams depicting mean fluorescence intensity (MFI) of CCR4 expression (black bars) or secondary antibody controls (gray bars) on indicated cells as determined by flow cytometry. Background fluorescence in secondary antibody-only samples (gray bars) is due to the enhanced autofluorescence of myeloid-derived cells. Asterisks denote significant differences between MFI of secondary antibody-only stained cells or MFI of cells stained with CCR4 Ab and secondary antibody; $^{**}P < 0.01$. Data shown are mean ± SEM of MFI as determined by flow cytometry (n = 3–4 mice). Data shown are representative of two independent experiments. (*C*) Quantitative analyses of histological stainings by immunohistochemistry of spinal cord sections from WT (squares, open bars) and $CCR4^{-/-}$ mice (diamonds, filled bars) stained with Luxol fast blue or mAbs against MAC-3, CD3, B220, and APP. Data are plotted as mean ± SE (n = 8 mice per group). (*D*) Diagram for absolute numbers of $CD4^+$ TCR^+ cells (pregated for $CD45^{high}$ expression) in WT (black bars) and $CCR4^{-/-}$ (white bars) mice as determined by flow cytometry (mean ± SE; diagram P = 0.0002; n = 12–13 mice per group). Data shown are representative of two independent experiments. (*E*) ELISpot analysis of CNS-isolated IFN-γ–producing MOG-reactive lymphocytes from MOG-immunized WT and $CCR4^{-/-}$ mice. Data shown are representative of two independent experiments. (*F*) Flow cytometry of CNS-isolated mononuclear cells from WT and $CCR4^{-/-}$ mice at peak disease. Shown are representative dot plots for expression of CD11b or MHC class II molecules and CD45 from one of three independent experiments, including at least three mice per group. Percentages of each cellular subset are included in the regional gates.

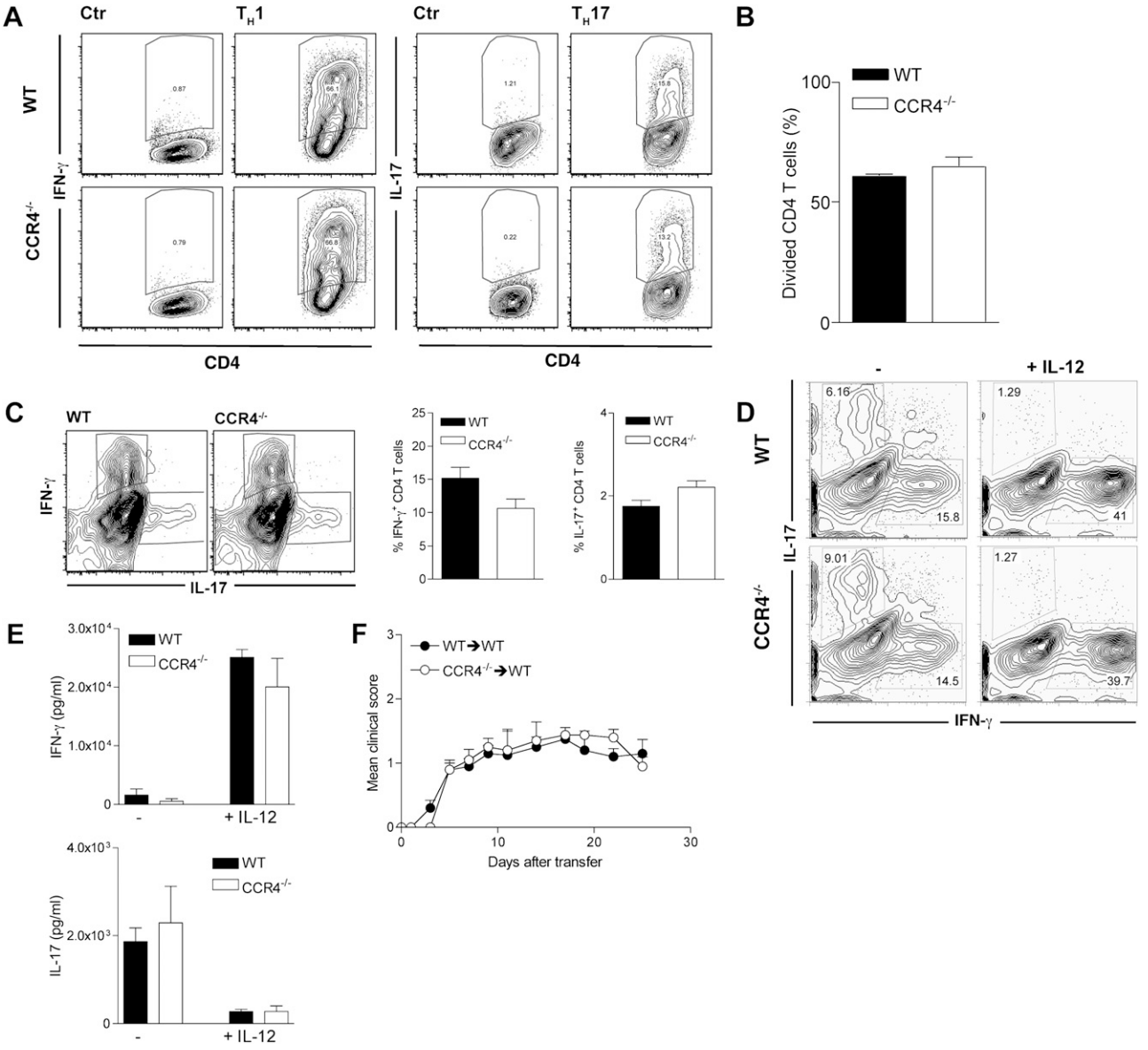

Fig. S2. Cytokine profiles in MOG-reactive WT and $CCR4^{-/-}$ CD4 T lymphocytes. (*A*) T_H-1 or T_H-17 differentiation in $CD4^+$ T cells in the absence of CCR4. Purified $CCR4^{-/-}$ or WT $CD4^+$ T cells were subjected to T_H-1 or T_H-17 differentiation protocols, and cytokine-producing $CD4^+$ T cells were determined by flow cytometry. Diagrams show mean percentages ± SEM of cytokine-producing cells (n = 4 mice per group). Data shown are representative for one of at least two independent experiments. (*B*) MOG-specific T-cell proliferation at the priming phase in $CCR4^{-/-}$ mice. Proliferation was assessed in CFSE-labeled $CD4^+$ T cells from day 10-immunized $CCR4^{-/-}$ or WT mice by flow cytometry. Diagram shows mean percentage ± SEM of CFSE-positive $CD4^+$ T cells that had undergone at least one division (n = 4 mice per group). Data shown are representative for one of two independent experiments. (*C*) IL-17 and IFN-γ production in the spleens at the priming phase in MOG-immunized $CCR4^{-/-}$ mice. Percentages of cytokine-producing $CD4^+$ T cells were determined by flow cytometry. (*Right*) Diagrams denote mean ± SEM of cytokine-producing cells (n = 4–5 per group). Data shown are representative for one of at least two independent experiments. (*D*) IL-17 and IFN-γ production in WT and $CCR4^{-/-}$ T lymphocytes after in vitro MOG restimulation in the presence or absence of IL-12. Splenocytes from day 10 MOG-immunized WT and $CCR4^{-/-}$ mice were cultured with MOG for 72 h in the presence or absence IL-12. Cytokine staining was determined by flow cytometry. Representative dot blots for WT (*Upper*) and $CCR4^{-/-}$ (*Lower*) T-lymphocyte cultures with quadrants for the respective cellular subsets are shown. Data shown are representative of at least two independent experiments. (*E*) ELISA of IFN- γ (*Upper*) and IL-17 levels (*Lower*) in the supernatants from cultures performed as described in *D*. Diagrams depict mean ± SEM of protein levels in supernatants. Data shown are representative of two independent experiments. (*F*) IL-17–producing $CCR4^{-/-}$ T lymphocytes induce equivalent albeit mild clinical EAE symptoms after transfer to naive WT recipients. T lymphocytes from day 10 MOG-immunized WT or $CCR4^{-/-}$ mice were cultured as described above and adoptively transferred in naïve WT mice. Shown is the clinical course of EAE induced in WT mice after adoptive transfer of MOG-reactive WT (●) or $CCR4^{-/-}$ (○) lymphocytes stimulated without IL-12 (n = 5 mice per group). Data shown are representative of two independent experiments.

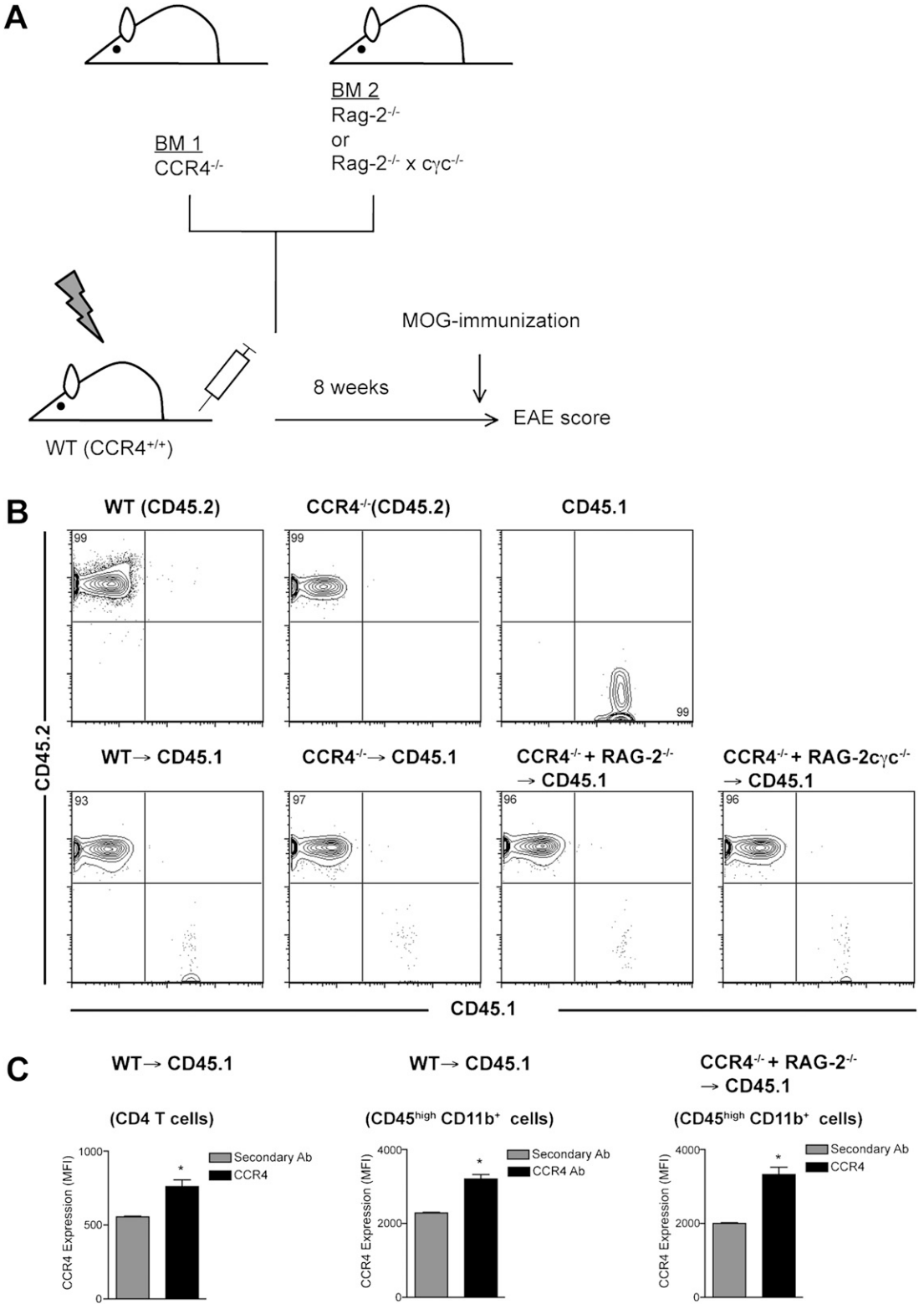

Fig. S3. Myeloid-derived cells expressing CCR4 are required for development of EAE. (*A*) Scheme of the generation of BM chimeric mice. (*B*) Shown are representative dot plots of control CD45.2 WT (*Upper Left*) and CD45.2 CCR4$^{-/-}$ (*Upper Center*) donor mice and WT CD45.1 (*Upper Right*) recipient mice. Lethally irradiated WT (CD45.1) recipients were reconstituted with BM from WT (*Lower Left*), CCR4$^{-/-}$ (*Lower Center Left*), CCR4$^{-/-}$ and RAG-2$^{-/-}$ (*Lower Center Right*), CCR4$^{-/-}$ and RAG-2-cγc knockout (*Lower Right*) BM cells. Flow cytometry of peripheral blood lymphocytes after staining with anti CD45.1 and CD45.2 antibodies of control mice and BM chimeras 7–8 wk after reconstitution. Frequencies of CD45.2 donor-derived cells are indicated in the respective quadrants of representative dot plots. Data show representative dot plots from one of two independent experiments (n = 12–13 chimeric mice per group). (*C*) CCR4 surface expression on CD4$^+$ T cells and CD11b$^+$ cells in BM chimeras. Shown are representative histograms of MFI of CCR4 expression (gray bars) or secondary Ab-only controls (black bars) on indicated cells as determined by flow cytometry. Data shown in the diagram are mean ± SEM for MFI of CCR4 expression on indicated cells as determined by flow cytometry (n = 3–4 mice per group). Data shown are representative for one of two independent experiments.

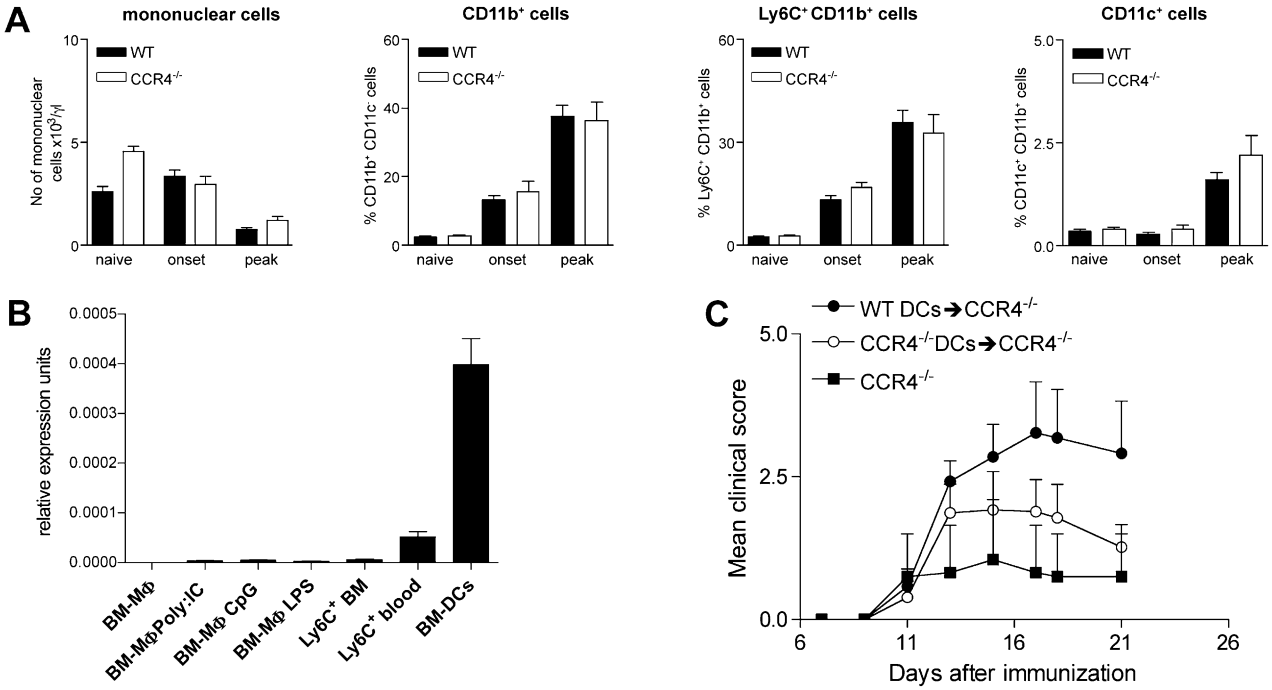

Fig. S4. CCR4$^{-/-}$ mice develop EAE after intracerebral injection of CCR4$^{+/+}$ DCs but not CCR4$^{-/-}$ DCs. (*A*) Flow cytometry of blood-derived mononuclear cells, macrophages, DCs, or Ly6C^{+} cells in naive WT and CCR4$^{-/-}$ mice or at the onset or peak of disease. Diagrams show absolute numbers of blood-derived lymphocytes, percentages of CD11b^{+} cells, Ly6C^{+} CD11b^{+}, or CD11c^{+} cells in WT (black bars) and CCR4$^{-/-}$ (white bars) mice (mean ± SEM; n = 4–5 mice per group). Data shown are representative for one of two independent experiments. (*B*) CCR4 mRNA expression in myeloid-derived cells. Real-time RT-PCR analysis for CCR4 mRNA levels in BMDCs, BM macrophages (BM-Mφ), and Ly6C^{+} cells from C57BL/6 mice. BM-Mϕ were stimulated with indicated TLR ligands. The relative mRNA expression normalized to GAPDH mRNA was determined and presented as mean ± SEM. Data shown are representative for one of two independent experiments. (*C*) CCR4$^{-/-}$ mice were MOG immunized and 8 d later intracerebrally microinjected with CCR4$^{+/+}$ MOG-loaded DCs (●) or CCR4$^{-/-}$ MOG-loaded DCs (○). Shown are mean clinical scores for each group of injected CCR4$^{-/-}$ mice and MOG-immunized CCR4$^{-/-}$ controls (■; n = 6–8 mice per group). Data shown are representative of two independent experiments.

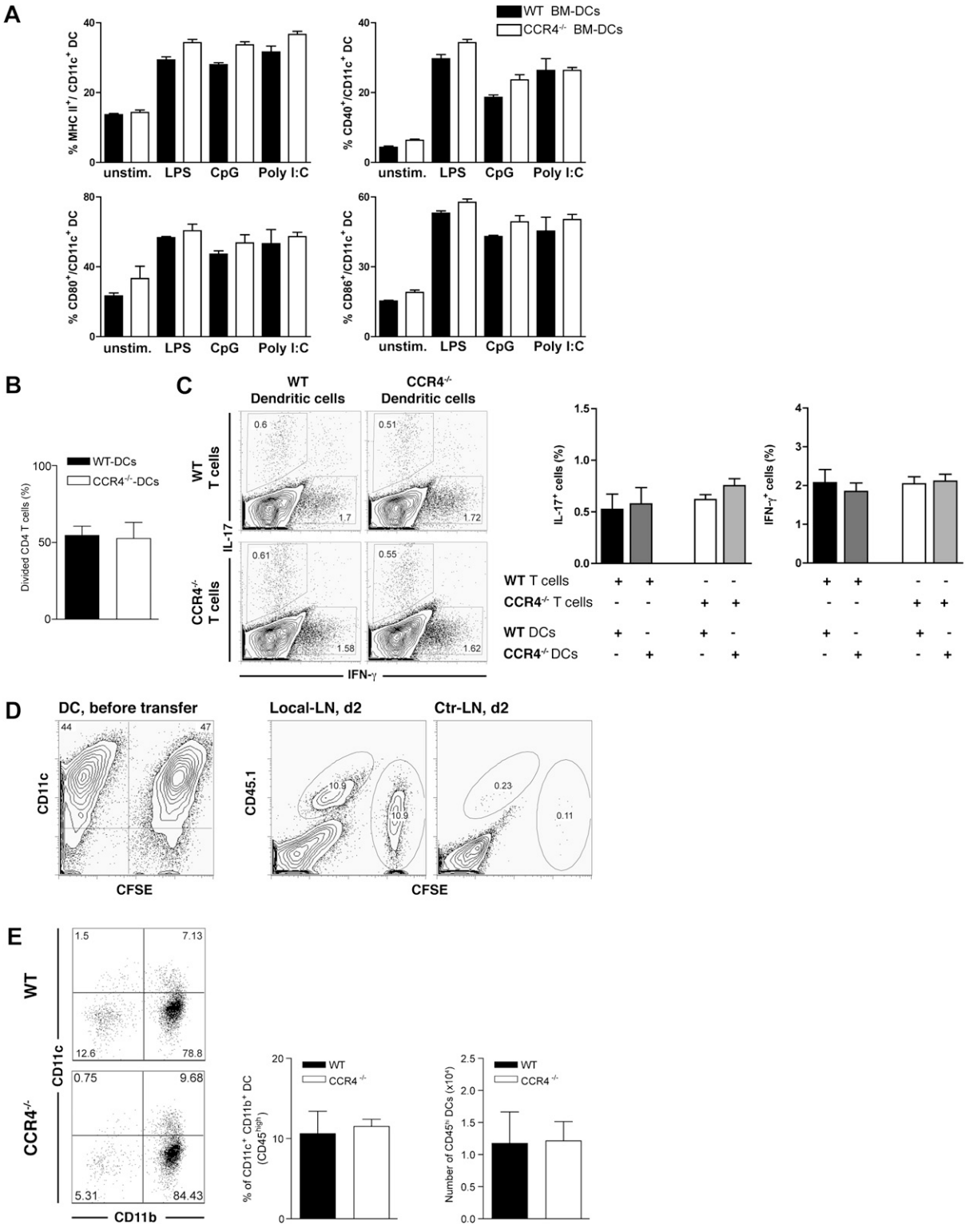

Fig. S5. CCR4$^{-/-}$ DCs are capable in maturation, T-cell priming, and in vivo migration from peripheral tissues into the lymph nodes. (*A*) Percentages of MHC class II^{+}, CD40^{+}, CD80^{+}, or CD86^{+} CD11c^{+} BMDCs from WT (black bars) and CCR4$^{-/-}$ (white bars) mice after stimulation with indicated TLR ligands. Data are mean ± SEM as determined by flow cytometry (n = 3–4 mice per group). Representative data from one of three experiments are shown. (*B*) CCR4$^{-/-}$ DCs are capable of inducing antigen-specific CD4^{+} T-cell proliferation. Proliferation was assessed in CFSE-labeled 2D2 T cells 72 h after culturing with MOG-loaded WT (black bar) or CCR4$^{-/-}$ DCs (white bar) by flow cytometry. Diagram shows mean percentage ± SEM of CFSE-positive 2D2 T cells that had undergone at least one division (n = 4 mice per group). Data shown are representative for one of two independent experiments. (*C*) Percentages of IL-17– and IFN-γ–producing MOG-reactive CD4^{+} T cells from WT (*Upper*) and CCR4$^{-/-}$ (*Lower*) mice after being rechallenged in vitro with MOG peptide-loaded WT (*Left*) or CCR4$^{-/-}$ BMDCs (*Right*). Data are mean ± SE; n = 6 MOG-immunized mice per group. Data shown are representative for one of two independent experiments. (*D*) In vivo migration of BMDCs from CCR4$^{-/-}$ mice. CFSE-labeled CCR4$^{-/-}$ BMDCs were mixed in a 1:1 ratio with C57BL/6 BMDCs (CD45.1) and transferred into RAG-2$^{-/-}$

Legend continued on following page

mice. Representative dot plots show flow cytometry of anti-mCD11c stained BMDC mix before transfer (*Left*), draining lymph nodes (*Center*), and nondraining lymph nodes (*Right*) of recipient mice 48 h later. BMDCs from C57BL/6 mice were identified by expression of CD45.1 and CCR4$^{-/-}$ BMDCs by CFSE by flow cytometry. Representative dot plots from one of three independent experiments with at least four mice in each experiment are shown. (*E*) Numbers of DCs in the CNS of WT and CCR4$^{-/-}$ mice at the onset of disease. Shown are representative dot plots (*Left*) of percentages of CD11c^{+} CD11b^{+} DCs or diagrams (*Right*) for percentages and absolute numbers of CD11c^{+} CD11b^{+} DCs (pregated for CD45^{hIgh} expression) in WT (black bars) and CCR4$^{-/-}$ (white bars) mice (mean ± SEM; *n* = 3–5 mice per group). Data shown are representative for one of two independent experiments.

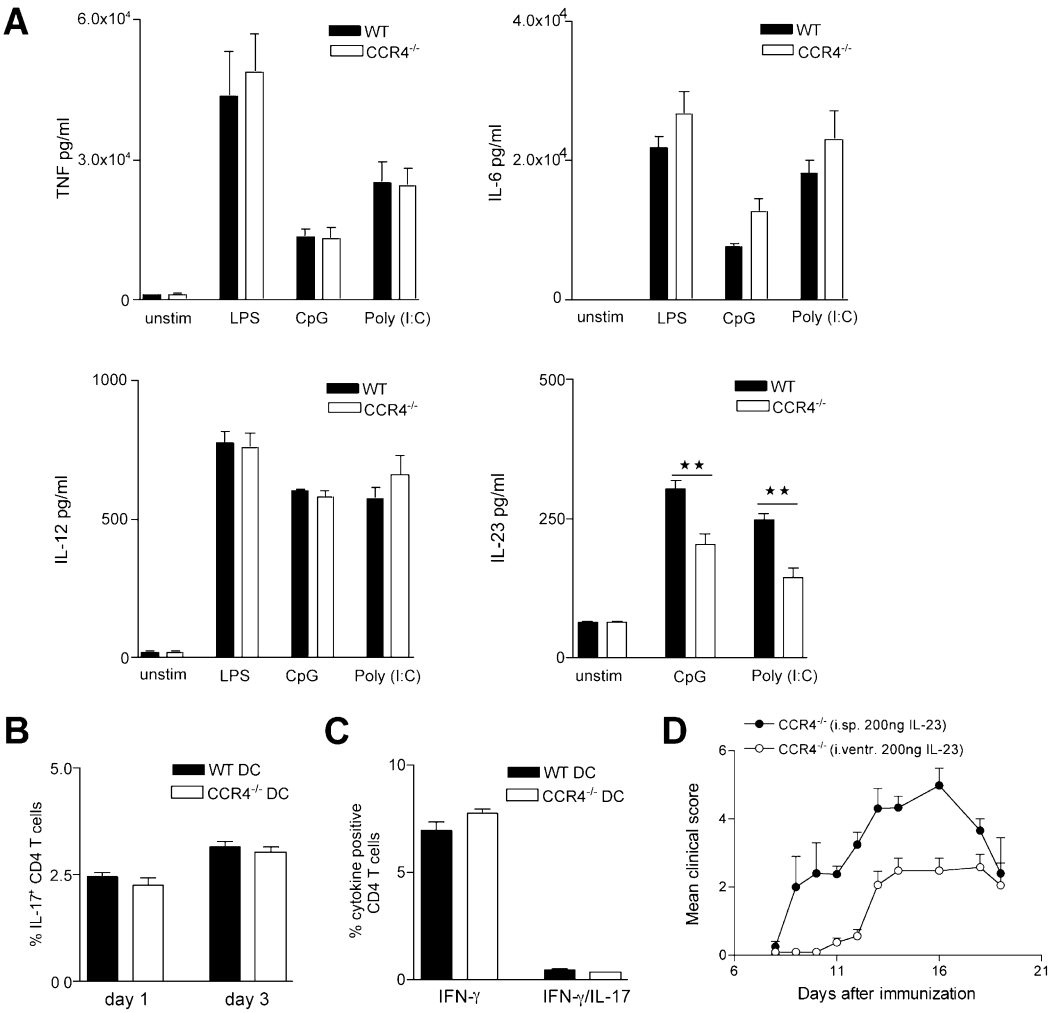

Fig. S6. CCR4$^{-/-}$ mice develop severe clinical EAE after intraspinal injection of IL- 23. (*A*) ELISA of TNF, IL-6, IL-12, and IL-23 production in BMDCs from WT (black bars) and CCR4$^{-/-}$ mice (white bars) after stimulation with TLR ligands. Data shown are mean ± SEM of cytokine levels in culture supernatants (*n* = 8 mice per group). Representative data of one of four independent experiments are shown. (*B*) Percentages of IL-17–producing MOG-reactive CD4^{+} T cells from WT (black bars) and CCR4$^{-/-}$ (white bars) mice after being rechallenged in vitro with MOG-peptide loaded WT or CCR4$^{-/-}$ BMDCs on day 1 and day 3. Data in the diagram are mean ± SE; *n* = 4–5 MOG-immunized mice per group. Data shown are representative for one of two independent experiments. (*C*) Percentages of IFN-γ– or IFN-γ/IL-17–producing MOG-reactive CD4^{+} T cells after in vitro rechallenge with MOG-loaded WT DCs or CCR4$^{-/-}$ DCs on day 4. Diagrams show mean ± SE of cytokine-producing cells; *n* = 4–5 MOG-immunized mice per group. Data shown are representative for one of two independent experiments. (*D*) CCR4$^{-/-}$ mice develop severe clinical EAE after intraspinal injection of IL-23. Shown are mean clinical scores for each group of MOG-immunized CCR4$^{-/-}$ mice injected with IL-23 either intraspinally (●) or intraventricularily (○; *n* = 6–8 mice per group). A representative experiment of two independent experiments is shown.

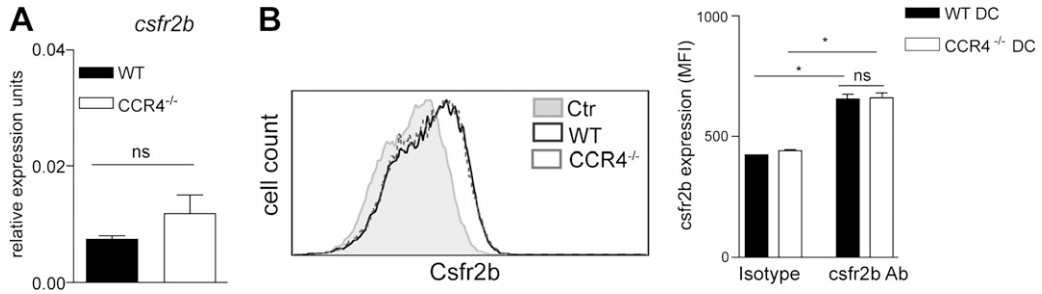

Fig. S7. Equivalent Csfr2b expression in CCR4$^{-/-}$ and WT DCs. (*A*) Real-time PCR analysis of csfr2b mRNA levels in BMDCs from WT and CCR4$^{-/-}$ mice. mRNA levels are normalized to β-actin expression, and results are presented as mean ± SEM (n = 3–5 mice per group). Data shown are representative for one experiment of two independent experiments. (*B*) Histograms show overlays for MFI of Csfr2b surface expression by BMDCs from WT (black line) and CCR4$^{-/-}$ (gray line) mice or isotype-stained control cells (gray shaded histogram). Histograms for MFI of Csfr2b in WT and CCR4$^{-/-}$ DCs are overlapping. Diagram shows MFI of Csfr2b surface expression on DCs from WT (black bars) and CCR4$^{-/-}$ (white bars) mice either isotype stained (*Left*) or stained with anti-Csfr2b Ab (mean ± SEM; n = 3–4 mice per group). Data shown are representative for one of two independent experiments.

Table S1. EAE incidence in WT and CCR4$^{-/-}$ mice

	WT	CCR4$^{-/-}$
No. of mice	29	32
Mean day of disease onset	9.8	10.3
Incidence of clinical signs (%)	25/29 (86%)	8/32 (25%)
Mean maximum clinical score for the group ± SE	3.16 ± 0.11	1.1 ± 0.08***
Mean maximum clinical score of EAE mice ± SE	3.54 ± 0.11	1.44 ± 0.09***

Results are a summary of three independent experiments.
***P < 0.001 vs. WT; Mann–Whitney U test.

Table S2. CCR4 signaling on hematopoietic cells controls EAE development

	WT→WT	CCR4$^{-/-}$→WT
No. of mice	8	11
Mean day of disease onset	10.25	7.00
Incidence of clinical signs (%)	8/8 (100%)	2/11 (18%)
Mean maximum clinical score for the group ± SE	4.3 ± 0.16	0.136 ± 0.05***
Mean maximum clinical score of EAE mice ± SE	4.4 ± 0.16	0.74 ± 0.12*

*P < 0.05; ***P < 0.001 vs. WT→WT; Mann–Whitney U test.